https://doi.org/10.5194/amt-2019-212
Preprint. Discussion started: 12 July 2019

Atmospheric Measurement Techniques Discussions

Performance Evaluation of THz Atmospheric Limb Sounder (TALIS) of China

Wenyu Wang[1,2], Zhenzhan Wang[1], Yongqiang Duan[1,2]

[1]Key Laboratory of Microwave Remote Sensing, National Space Science Center, Chinese Academy of Sciences, Beijing, China
[2]University of Chinese Academy of Sciences, Beijing, China

Correspondence to: Zhenzhan Wang (wangzhenzhan@mirslab.cn)

Abstract. THz Atmospheric Limb Sounder (TALIS) is a microwave limb sounder being developed for atmospheric high precision observation by the National Space Science Center, Chinese Academy of Sciences (NSSC, CAS). It is designed to measure the temperature and chemical species such as O_3, HCl, ClO, N_2O, NO, NO_2, HOCl, H_2O, HNO_3, HCN, CO, SO_2, BrO, HO_2, H_2CO, CH_3Cl, CH_3OH, and CH_3CN with high vertical resolution from surface to about 100 km to improve our comprehension of atmospheric chemistry and dynamics, and to monitor the man-made pollution in the atmosphere. Four heterodyne radiometers including several FFT spectrometers of 2 GHz bandwidth with 2 MHz resolution are employed to obtain the atmospheric thermal emission in broad spectral regions centred near 118, 190, 240, and 643 GHz. A theoretical simulation is performed to estimate the retrieval precision of the main targets. Single scan measurement and averaged measurement are considered in simulation, respectively. Temperature profile can be obtained with the precision of < 2K for a single scan from 15 to 85 km by using 118 GHz radiometer, and the 240 and 643 GHz radiometer can provide temperature information in the upper troposphere. Chemical species such as H_2O, O_3, HCl, N_2O, and HNO_3 show high single scan retrieval precision of 1–50% at most altitudes. The other species should be retrieved by using averaged measurements because of the weak intensity or low abundance.

1 Introduction

High precision observation of the Earth's atmosphere is essential to the numerical weather prediction and climate change studies. The satellite can provide global coverage atmospheric monitoring in a short time. Instruments such as nadir microwave sounder and infrared sounder have been applied to measure the atmospheric temperature and humidity but with the poor vertical resolution and altitude range (Swadley et al., 2008). Terahertz limb sounder can not only provide the temperature profile with better vertical resolution but gather information on chemical composition in a wide altitude range and independent of the day-night cycle. Microwave limb sounding is a particularly useful technique in detecting stratospheric and mesospheric temperature and chemistry, and also has large potential for global wind measurement in the middle and upper atmosphere (Ochiai et al., 2017).

https://doi.org/10.5194/amt-2019-212
Preprint. Discussion started: 12 July 2019

Atmospheric Measurement Techniques Discussions

A few instruments have been launched in recent twenty years, their observation data have offered a better understanding of the physical and chemical processes in the Earth' atmosphere. The first instrument applying the microwave limb sounding technique from space was the Microwave Limb Sounder (MLS) onboard the Upper Atmosphere Research Satellite (UARS) launched in 1991. The sounder offered unique information of temperature/pressure, O_3, H_2O, ClO, and additional data products including SO_2, HNO_3, and CH_3CN (Waters et al., 1993). The Sub-Millimetre Radiometer (SMR) onboard the Odin satellite launched in February 2001 was the first radiometer to employ sub-millimetre in limb sounding. Various target species such as O_3, ClO, N_2O, HNO_3, H_2O, CO, NO, as well as isotopes of H_2O, O_3, and ice cloud have been detected (Murtagh et al., 2002; Urban et al., 2005; Eriksson et al., 2007). EOS MLS, the follow-on of UARS MLS onboard the Aura satellite launched in July 2004 gave successful observations of OH, HO_2, H_2O, O_3, HCl, ClO, HOCl, BrO, HNO_3, N_2O, CO, HCN, CH_3CN, SO_2, ice cloud, and wind (Waters et al., 2004; Waters et al., 2006; Wu et al., 2008; Livesey et al., 2013). The Superconducting Submillimeter-wave Limb-Emission Sounder (SMILES) onboard the Japanese Experiment Module (JEM) of the International Space Station (ISS) launched in September 2009 (Kikuchi et al., 2010). SMILES was equipped with 4K cooled Superconductor–Insulator–Superconductor (SIS) mixers to reduce the system noise temperature so that the sensitivity of the SMILES was higher than that of other similar sensors such as MLS and SMR (Takahashi et al., 2010; Baron et al., 2011). Currently, several new instruments are being developed. THz limb sounder (TLS) proposed in the US aims to measure lower thermospheric wind, oxygen density, and temperature (Wu et al., 2016). However, it cannot obtain the information in the stratosphere and lower mesosphere. Stratospheric Inferred Winds (SIW) is a Swedish mini sub-millimetre limb sounder for measuring wind, temperature, and molecules in the stratosphere. It can provide horizontal wind vectors within 30–90 km, as well as the profiles of temperature, O_3, H_2O and other abundant chemical species (Baron et al., 2018). TLS and SIW are designed for small satellites and will be launched as early as 2020–2022. In addition, the follow-on of SMILES, SMILES-2, is being studied for measuring the whole vertical range of 15−180 km with low noise (Ochiai et al., 2017).

THz Atmospheric Limb Sounder (TALIS) is being designed at National Space Science Center, the Chinese Academy of Sciences (NSSC, CAS) for high precision measurement of atmospheric temperature and key chemical species. It has four microwave radiometers in the frequency bands of 118, 190, 240, and 643 GHz which are similar to EOS MLS. TALIS mission objectives are to provide the information for research on the dynamics and the chemistry of the middle and upper atmosphere by measuring the volume mixing ratio (VMR) profile of the chemical species and other atmospheric condition such as cirrus with much finer spectrum resolution.

In this paper, we present a simulation study on precision estimates for the geophysical parameters measured by TALIS. The outline of the present study is as follows: Section 2 describes the instrument characteristics and spectral bands. The retrieval method and the simulation result are discussed in Sects. 3 and 4, respectively. The final section gives a conclusion about the performance.

https://doi.org/10.5194/amt-2019-212
Preprint. Discussion started: 12 July 2019

Atmospheric Measurement Techniques Discussions

2 Instrument overview

2.1 Instrument characteristics

The TALIS instrument will be set at a sun-synchronous orbit at a normal altitude of 600 km. The antenna will scan the limb vertically from surface to about 100 km with an integration time of 0.1 s. The signals from the antenna will be feed into the mixers. Single-sideband (SSB) can keep the complete spectral lines while double-sideband (DSB) can cover more spectral lines because of the image band. Thus, all the radiometers of TALIS will operate in the double-sideband mode except the 118 GHz radiometer. Eleven FFT spectrometers of 2 GHz bandwidth with 2 MHz resolution will be used in TALIS. TALIS has four radiometers which cover the significant thermal emission spectra in the 118, 190, 240, and 643 GHz regions. The proposed characteristics of the TALIS payload which may be slightly modified in the future are summarized in Table 1.

Table 1. Characteristics of the TALIS payload

Radiometer	Frequency (GHz)	Target species	T_{sys} (K)	Radiometer	Frequency (GHz)	Target species	T_{sys} (K)
118 GHz	117.75–119.75	Temperature, pressure	800	240 GHz	229.66–231.66 247.66–249.66	O_3, HNO_3, CO, NO_2, SO_2, temperature, pressure	1000
190 GHz	175.5–177.5 202.7–204.7	H_2O, N_2O, HCN, ClO, O_3, SO_2	1000		232.16–234.16 245.16–247.16		
	178.9–180.9 199.3–201.3				234.66–236.66 242.66–244.66		
	183.0–185.0 195.2–197.2			643 GHz	624.47–626.47 659.27–661.27	HCl, N_2O, ClO, CH_3Cl, HO_2, BrO, HOCl, NO, CO, SO_2, O_3, HNO_3, H_2O, H_2CO, CH_3CN, CH_3OH, temperature, pressure	3000
					627.37–629.37 656.37–658.37		
					632.37–634.37 651.37–653.37		
					634.87–636.87 648.87–650.87		

2.2 Bands selection

The spectral bands of TALIS are selected with the following criterions: (1) maximizing the number of species which will exert a strong influence on atmospheric chemistry and dynamics, (2) necessary space between the passband, (3) trade-off between realizable bandwidth and resolution. TALIS covers most spectral bands of EOS MLS and extends them. The broader bandwidth, finer resolution, and lower noise of TALIS can provide higher retrieval precision and effective altitude range compared with EOS MLS. More chemical species can be measured by TALIS, such as NO_2, NO, H_2CO, and SO_2 (normal concentration).

The 118 GHz radiometer, covering the strong O_2 line at 118.75 GHz, is used to measure the atmospheric temperature and tangent pressure. Since there are few meteorological data set about the temperature above the middle atmosphere with

https://doi.org/10.5194/amt-2019-212
Preprint. Discussion started: 12 July 2019


Atmospheric Measurement Techniques Discussions

good vertical resolution, it is necessary to measure the temperature profile with wide altitude range, good vertical resolution, and high precision. Other information such as ice cloud can be treated as additional measurement. Figure 1 gives an overview of the 118 GHz spectral band.

The 190 GHz radiometer is mainly designed to cover the 183.31 GHz H_2O line. Monitoring water vapour is important for understanding the mechanisms that humidity feedback on climate, and is essential for improving the accuracy of the weather forecast. Other chemical species such as N_2O, ClO, O_3, and HCN are also included in 190 GHz bands (see Fig. 2).

The main objective of the 240 GHz radiometer is to measure the CO at 230.54 GHz and the strong O_3 lines in a wide spectral band where upper tropospheric O_3 can be obtained with high precision because of the weak water vapour continuum absorption. In addition, the 233.95 GHz O_2 line will be used to measure temperature and tangent pressure together with 118.75 GHz line. SO_2 is an important pollutant in the Earth' atmosphere and will give rise to acid rain. There is no obvious SO_2 emission with the standard profile present in the passband of 240 GHz radiometer. However, MLS demonstrated that SO_2 can be measured by 240 GHz radiometer cooperated with 190 GHz radiometer when its concentration significantly enhanced above nominal background such as volcano eruption (Pumphrey et al., 2015). The wide and stable lines of HNO_3 can be used to retrieve profile well. NO_2 is a unique species not covered by EOS MLS. The spectra of 240 GHz radiometer are depicted in Fig. 3.

The 643 GHz radiometer is designed to cover as more spectral lines as possible, thus about 17 species are included. The spectral lines covering O_3, HCl, ClO, N_2O, O_2, and H_2O are clearly visible (Fig. 4), and other lines which are relatively weak such as NO, HNO_3, CO, SO_2, BrO, HO_2, H_2CO, HOCl, and CH_3Cl, can also be used. The O_2 line at 627.75 GHz and the H_2O line at 657.9 GHz have the potential to be used as supplements to 118 and 190 GHz radiometers. O_3 is the major species in the stratosphere and mesosphere, which is quite important in atmospheric radiation transfer. Using the high sensitivity lines in the 643 GHz bands can measure O_3 with high precision (Takahashi et al., 2011; Kasai et al., 2013). The only lines of HCl below 1 THz are in the 625 GHz frequency band, thus HCl can be measured by 643 GHz radiometer. ClO is a key catalyst for ozone loss and the 649.45 GHz line is suitable for ClO observation with good precision (Santee et al., 2008; Sato et al., 2013). The HOCl, which will affect stratospheric chlorine budget, has distinct lines above 600 GHz, and the 635.87 GHz line has been pointed out to be the best line for observation (Urban, 2003). Both 649.701 and 660.486 GHz lines can be used to measure the hydroperoxyl radical HO_2, which will contribute to the catalytic ozone chemistry in the upper stratosphere and mesosphere (Millán et al., 2015). Since ClO, HO_2, and HOCl all can be measured, the reaction rate of ClO and HO_2 to form HOCl in the atmosphere can be determined (Johnson et al., 1995). N_2O can be measured at 652.834 GHz, which has been validated by MLS (Lambert et al., 2008). NO has two weak signals at 651.45 and 651.75 GHz which can be used to measure the abundance. HNO_3 can be measured using 650 GHz bands. Measuring these nitrogen species will help researchers to understand the chemistry and dynamics of the atmosphere better. The BrO, which plays an important role in the depletion of ozone, can be measured using 624.768 and 650.179 GHz lines. Because of the low abundance of BrO, measurements must be significantly averaged in order to get reliable results (Millán et al., 2012). CO and H_2CO are the

https://doi.org/10.5194/amt-2019-212
Preprint. Discussion started: 12 July 2019

Atmospheric Measurement Techniques Discussions

major species in the CH_4 oxidation to CO_2 and H_2O in the stratosphere and mesosphere (Suzuki et al., 2015). The major spectral line of CO used by MLS is at 230.538 GHz, however, the 661.07 GHz line can also provide information (Livesey et al., 2008). H_2CO has a line at 656.45 GHz, but the signal is very weak. The SO_2 lines in the 660 GHz band can be used to detect the background levels of SO_2. CH_3Cl can be measured in the 649 GHz band near the line of ClO. MLS measured CH_3OH in the troposphere and lower stratosphere because of the negative bias in ClO retrieval, and measured CH_3CN by 625 GHz spectrometer (Pumphrey et al., 2011).

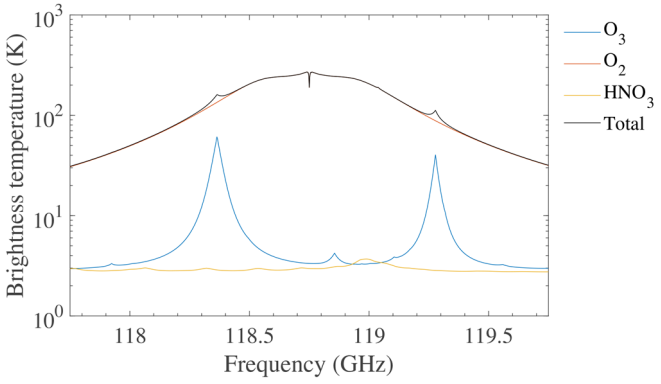

Figure 1. Contributions of the main target chemical species to the 118 GHz spectrum. The brightness temperature is measured from single sideband radiometer. The tangent height is 30 km.

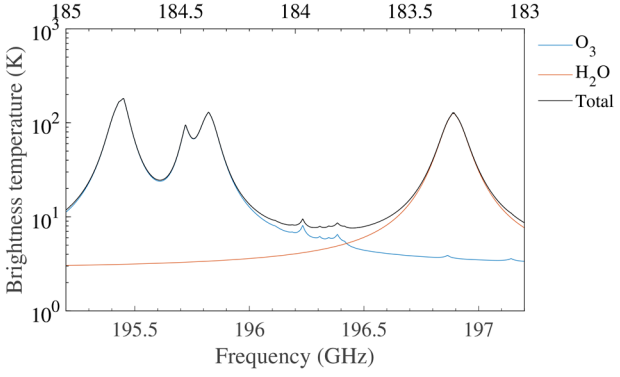

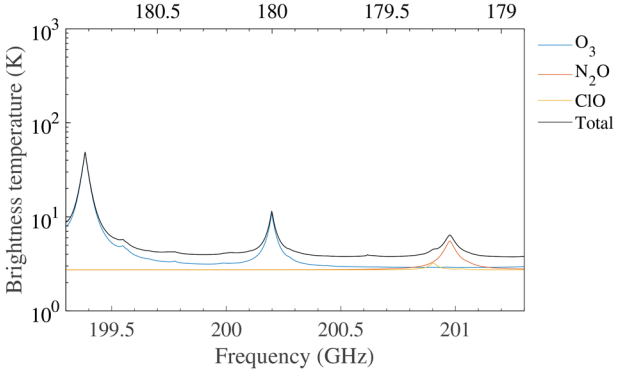

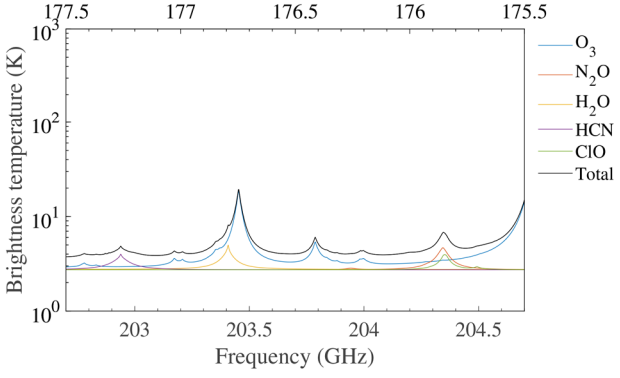

https://doi.org/10.5194/amt-2019-212
Preprint. Discussion started: 12 July 2019

Atmospheric Measurement Techniques Discussions

Figure 2. Contributions of the main target chemical species to the 190 GHz spectra. The brightness temperature is measured from double sideband radiometer. The tangent height is 30 km. The top axis represents the lower sideband frequencies and the bottom axis represents the upper sideband frequencies. Each panel represents a single spectrometer.

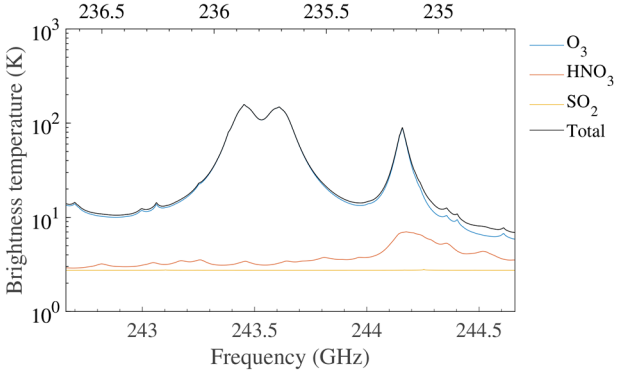

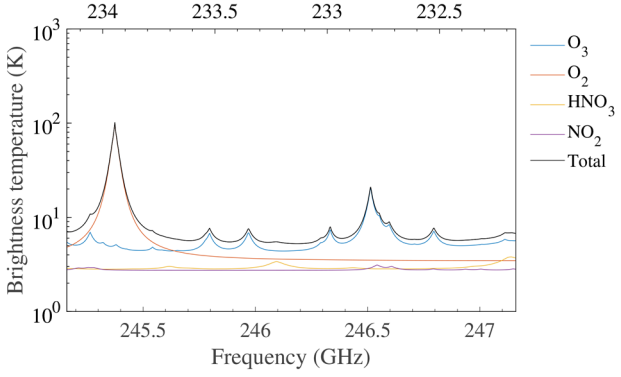

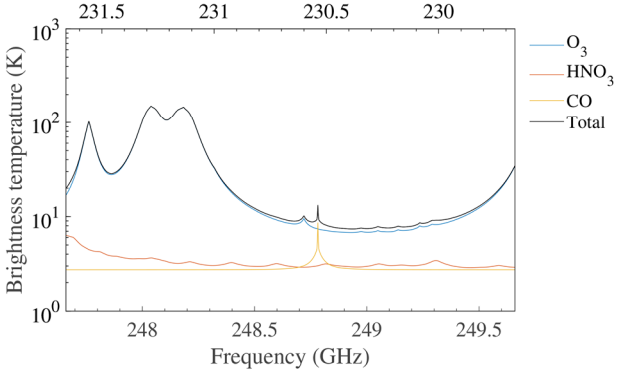

Figure 3. Contributions of the main target chemical species to the 240 GHz spectra. The brightness temperature is measured from double sideband radiometer. The tangent height is 30 km. The top axis represents the lower sideband frequencies and the bottom axis represents the upper sideband frequencies. Each panel represents a single spectrometer.

https://doi.org/10.5194/amt-2019-212
Preprint. Discussion started: 12 July 2019

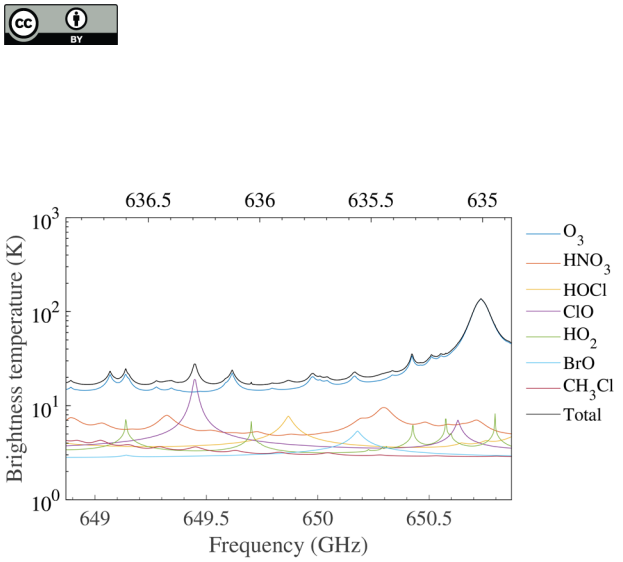

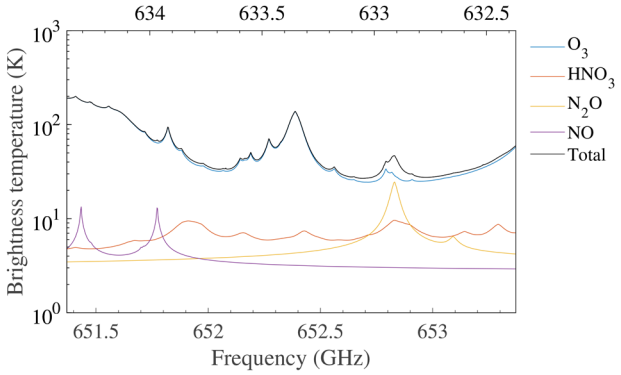

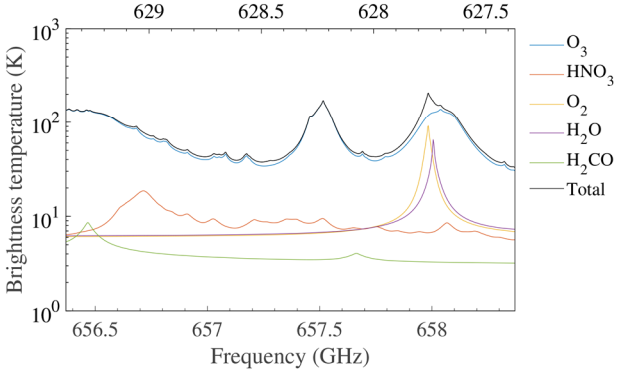

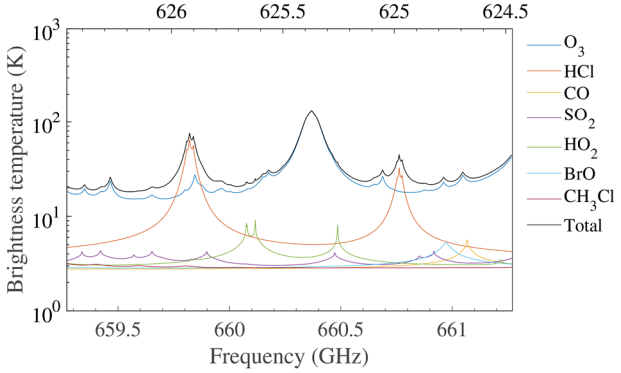

Figure 4. Contributions of the main target chemical species to the 643 GHz spectra. The brightness temperature is measured from double sideband radiometer. The tangent height is 30 km. The top axis represents the lower sideband frequencies and the bottom axis represents the upper sideband frequencies. Each panel represents a single spectrometer.

3 Retrieval methodology

3.1 Forward model

The retrieval of data measured by microwave limb sounder requires the accurate simulation of the observed thermal emission spectra. The forward model is a mathematical tool used to describe the radiative transfer, spectroscopy, and instrumental characteristics. The output of the forward model is the convolution of atmospheric radiation and instrument response.

Radiative transfer describes the emission, propagation, scattering, and absorption of electromagnetic radiation (Mätzler., 2006). The complete radiative transfer equation can be expressed as

$$\frac{dI_v(s)}{ds} = -k(s)I_v(s) + \alpha(s)B_v(s) + \frac{k(s)}{4\pi}\int_{4\pi} p(\theta,\phi,\theta',\phi')I_v(s,\theta',\phi')d\Omega', \quad (1)$$

https://doi.org/10.5194/amt-2019-212
Preprint. Discussion started: 12 July 2019


Atmospheric Measurement Techniques Discussions

$I_v(s)$ is the radiance at frequency v reaching the sensor and k is the extinction coefficient containing contributions from absorption and scattering. α is the absorption coefficient and B_v stands for the atmospheric emission which is given by Planck function describing the radiation of a black-body at temperature T and frequency v per unit solid angle, unit frequency interval and unit emitting surface (Urban et al., 2004):

$$B_v(T) = \frac{2hv^3}{c^2}\frac{1}{e^{hv/k_BT}-1}, \quad (2)$$

where h is the Planck constant, c is the speed of light, k_B denotes Boltzmann constant. Thus, the radiance can be converted to the brightness temperatures. The so-called phase function p describes the transfer of the radiance from the direction (θ, ϕ) to the direction (θ', ϕ') of the considered propagation path.

Spectroscopy is the method to calculate the absorption coefficient which requires pressure, temperature, and the species concentrations along the line of sight. The basic expression can be written as:

$$\alpha(v) = nS(T)F(v), \quad (3)$$

where S is called the line strength, F means the line shape function, and n is the number density of the absorber.

Scattering usually can be neglected above the upper troposphere because of the cloud free. In this way and assuming Local Thermodynamic Equilibrium (LTE), the formal solution of the radiative transfer equation is defined by

$$I_v(S_2) = I_v(S_1)e^{-\tau_{v(S_1,S_2)}} + \int_{S_1}^{S_2} \alpha_v(s)B_v(T)e^{-\tau_{v(S,S_2)}}ds, \quad (4)$$

where τ is the opacity or optical thickness.

Sensor characteristics also have to be taken into account by the forward model, including the antenna field-of-view, the sideband folding, and the spectrometer channel response (Eriksson et al., 2006).

Firstly, the radiance which encounters the antenna response could be expressed by the integration:

$$I_v^a = \int_\Omega I_v(\Omega)W_v^a(\Omega)d\Omega, \quad (5)$$

where W_v^a is the normalized antenna response function. Normally, the variation of I_v in azimuth angle dimension can be neglected or calculated before-hand. Secondly, a heterodyne mixer needs to convert the signals to intermediate frequency, which will lead to a consequence that the lower and upper sideband are folded. The apparent intensity after the mixer can be modelled as:

$$I_v^{if} = \frac{W_v^s(v)I_v^a + W_v^s(v')I_{v'}^a}{W_v^s(v) + W_v^s(v')}, \quad (6)$$

where W_v^s means the sideband response. At last, the final signal will be recorded by spectrometers, which can be described by a similar way as the antenna response:

$$I^c = \int_v I_v^{if} W_v^c(v)dv. \quad (7)$$

Here W_v^c means the normalized channel response, and the radiance is denoted I^c.

https://doi.org/10.5194/amt-2019-212
Preprint. Discussion started: 12 July 2019


Atmospheric Measurement Techniques Discussions

3.2 Retrieval algorithm

Optimal estimation method (OEM) is the most common method used in atmospheric sounding for retrieving vertical profiles of chemistry species (Rodgers, 2000).

In OEM theory, a predicted noisy measurement $\hat{\boldsymbol{y}}$ can be expressed by a forward model $\boldsymbol{F}$ with an unknow atmospheric state $\boldsymbol{x}$ and the system noise ϵ_y according to:

$$\hat{\boldsymbol{y}} = \boldsymbol{F}(\boldsymbol{x}, \boldsymbol{b}) + \epsilon_y. \tag{8}$$

The predicted radiance $\hat{y}$ are compared with the observed radiance y so that the unknow state which minimize the cost function χ^2 could be found. The cost function is given by:

$$\chi^2 = [\boldsymbol{y} - \boldsymbol{F}(\boldsymbol{x}, \boldsymbol{b})]^T \boldsymbol{S}_y^{-1} [\boldsymbol{y} - \boldsymbol{F}(\boldsymbol{x}, \boldsymbol{b})] + [\boldsymbol{x} - \boldsymbol{x}_a]^T \boldsymbol{S}_a^{-1} [\boldsymbol{x} - \boldsymbol{x}_a], \tag{9}$$

where x_a is a priori state vector, $\boldsymbol{S}_a$ and $\boldsymbol{S}_y$ stand for the covariance matrices representing the natural variability of the state vector and the measurement error vector, respectively. Assuming there is no correlation between channels, the off-diagonal elements of $\boldsymbol{S}_y$ are zero and the diagonal elements are set to the square of the system noise. Usually, a simple formula can be used to determine the radiometric noise standard deviation:

$$\epsilon = \frac{T_{rec} + T_A}{\sqrt{\beta\, d\tau}}, \tag{10}$$

where T_{rec} is the system noise temperature and T_A is the antenna temperature. β is the noise equivalent bandwidth and $d\tau$ is the integration time for measuring a single spectrum. A more accurate formula is commonly represented by (Bremer, 1979):

$$\epsilon = (T_{rec} + T)\sqrt{\frac{1}{\beta\, d\tau} + \left(\frac{\Delta G}{G}\right)^2}, \tag{11}$$

where the $\Delta G \,/\, G$ describe the correlated noise from the gain variations along the signal path. The diagonal elements of the S_a specify a priori variance and the off-diagonal terms is used to describe correlations between adjacent elements in order to make the retrieved profile smoother.

Finally, the Levenberg–Marquardt method which is the modification of the Gauss-Newton iterative is used to solve the nonlinear problem. The solution is given by

$$\boldsymbol{x}_{i+1} = \boldsymbol{x}_i + \left[(\boldsymbol{I} + \gamma)\boldsymbol{S}_a^{-1} + \boldsymbol{K}_{xi}{}^T \boldsymbol{S}_y^{-1} \boldsymbol{K}_i\right]^{-1} \left\{\boldsymbol{K}_{xi}{}^T \boldsymbol{S}_y^{-1} [\boldsymbol{y} - \boldsymbol{F}(x_i)] - \boldsymbol{S}_a^{-1} (\boldsymbol{x}_i - \boldsymbol{x}_a)\right\}, \tag{12}$$

where γ denotes the Levenberg–Marquardt parameter, and $\boldsymbol{K}_{xi}$ represents the weighting function matrix (Jacobian).

The OEM method provides a strict approach to analyse the retrieval results. The averaging kernel matrix $\boldsymbol{A}$, which represent the sensitivity of the retrieved state to the true state, is written as:

$$\boldsymbol{A} = \boldsymbol{G}_y \boldsymbol{K}_x = \frac{\partial \hat{\boldsymbol{x}}}{\partial \boldsymbol{x}}, \tag{13}$$

where the G_y is the contribution matrix, which express the sensitivity of the retrieved state to the measurement:

$$\boldsymbol{G}_y = \frac{\partial \hat{\boldsymbol{x}}}{\partial \boldsymbol{y}} = \left(\boldsymbol{K}_x{}^T \boldsymbol{S}_y \boldsymbol{K}_x + \boldsymbol{S}_a^{-1}\right)^{-1} \boldsymbol{K}_x{}^T \boldsymbol{S}_y^{-1}. \tag{14}$$

https://doi.org/10.5194/amt-2019-212
Preprint. Discussion started: 12 July 2019


Atmospheric Measurement Techniques Discussions

The retrieval resolution can be estimated from the full width at half-maximum (FWHM) of the averaging kernel (Marks and Rodgers, 1993).

There is another useful variable defined as measurement response, which represents the true state contribution in the retrieval (Baron et al., 2002):

$$W(i) = \sum_j |A(i,j)|. \quad (15)$$

The ideal measurement response should be near 1. In practice, reliable range of a retrieval is usually characterised by $|W - 1| < 0.2$.

The total retrieval error can be described by three covariance matrices, the smoothing error covariance matrix which is from the need of a priori information:

$$\boldsymbol{S}_n = (\boldsymbol{A} - \boldsymbol{I})\boldsymbol{S}_a(\boldsymbol{A} - \boldsymbol{I})^T, \quad (16)$$

the measurement error covariance matrix due to the measurement noise:

$$\boldsymbol{S}_m = \boldsymbol{G}_y \boldsymbol{S}_y {\boldsymbol{G}_y}^T, \quad (17)$$

and the model parameter error covariance matrix introduced by the uncertainties in the forward model:

$$\boldsymbol{S}_s = \boldsymbol{G}_y \boldsymbol{K}_b \boldsymbol{S}_b \boldsymbol{G}_y {\boldsymbol{K}_b}^T. \quad (18)$$

4 Measurement performance

4.1 Simulation setup

The objective of the simulation is to evaluate the observation performance of TALIS and give advice for further modification. In this simulation, the forward model Atmospheric Radiative Transfer Simulator (ARTS 2.3) and its corresponding retrieval tool Qpack2 are used (Eriksson et al., 2005; Eriksson et al., 2011). The instrumental setup follows the characteristics of TALIS described in Table 1. Brightness temperature measurements would be made in four spectral bands which are discussed in Sect.2. The ideal rectangle channel response function is used. The scan altitude range is from 10 to 95 km and the vertical separation is assumed to be 2.5 km. It is the trade-off between the step of efficient limb observation and the optimum information can be obtained (Livesey and Snyder, 2004). Pressure vertical coordinate is used in retrieval.

A mid-latitude summer atmospheric condition (profiles of BrO and HO_2 are from MLS L3 data) is chosen to perform the simulation. The scattering from tropospheric clouds, refraction, and Zeeman effect are not considered because of the large computational complexity. A spectroscopic line parameters catalogue created with the data taken from JPL catalogue (Pickett et al., 1998), HITRAN database (Rothman et al., 2013), and Perrin catalogue (Perrin et al., 2005) is used for line-by-line absorption calculation. The measurement covariance matrix is set diagonal as described in Sect.3 in order to reduce the computing time. 100% of a typical profile is used to build the a priori covariance matrix with 3 km vertical correlation between the adjacent pressure levels by a parametric Gaussian function. The true profiles are perturbed to be the a priori profiles. The species profiles are multiplied by a factor of 1.1, and the temperature profile is added a 5 K offset.

https://doi.org/10.5194/amt-2019-212
Preprint. Discussion started: 12 July 2019


Atmospheric Measurement Techniques Discussions

The expected 1σ noise is calculated by Eq. (10) for convenience, and it should be divided $\sqrt{2}$ when considering the double sideband radiometers. Therefore, the noise is assumed to be 2 K, 1.7 K, 1.7 K, and 5 K, respectively. The species such as BrO and HO_2 which emission radiances are small compared with the system noise must be averaged to increase the precision. Here the lower noise (1σ noise multiply a factor of 0.1) is used to represent the averaged production.

4.2 Retrieval precision

Since the simulation has been performed, an evaluation of the retrieval precision on the target species of TALIS is made. Retrieval profile, a priori profile, and true profile are all plotted in the figures. The precision (square root of diagonal elements of the error covariance matrix) is given for a single scan and averaged measurement respectively, and the relative error is also provided. Auxiliary information about averaging kernel function and measurement response are also included in the figures. Results are discussed in details in the followings.

4.2.1 High precision products

Temperature, H_2O, O_3, HNO_3, HCl, N_2O, and ClO are treated as high precision products because of the good precision for a single scan measurement. These products can be used in scientific research directly.

Atmospheric temperature is the most important parameter that can be retrieved with high signal-noise ratio in lower frequency or good vertical resolution in high frequency by using O_2 lines. TALIS will use the 118 GHz radiometer to detect atmospheric temperature profile, with 240 and 643 GHz radiometers worked as supplements in the upper troposphere. Results are shown in Fig. 5, the sensitivity is significantly high at the 118 GHz band. Single scan precision is < 1K from 25 to 45 km, < 2K below 80 km. The precision of averaged measurement will be < 1K from 15 to 85 km. Retrieval precision of 240 GHz is better in the upper troposphere compared with that of 118 GHz. Result of 643 GHz seems not very good.

https://doi.org/10.5194/amt-2019-212
Preprint. Discussion started: 12 July 2019

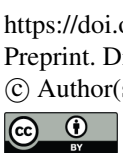

Atmospheric Measurement Techniques Discussions

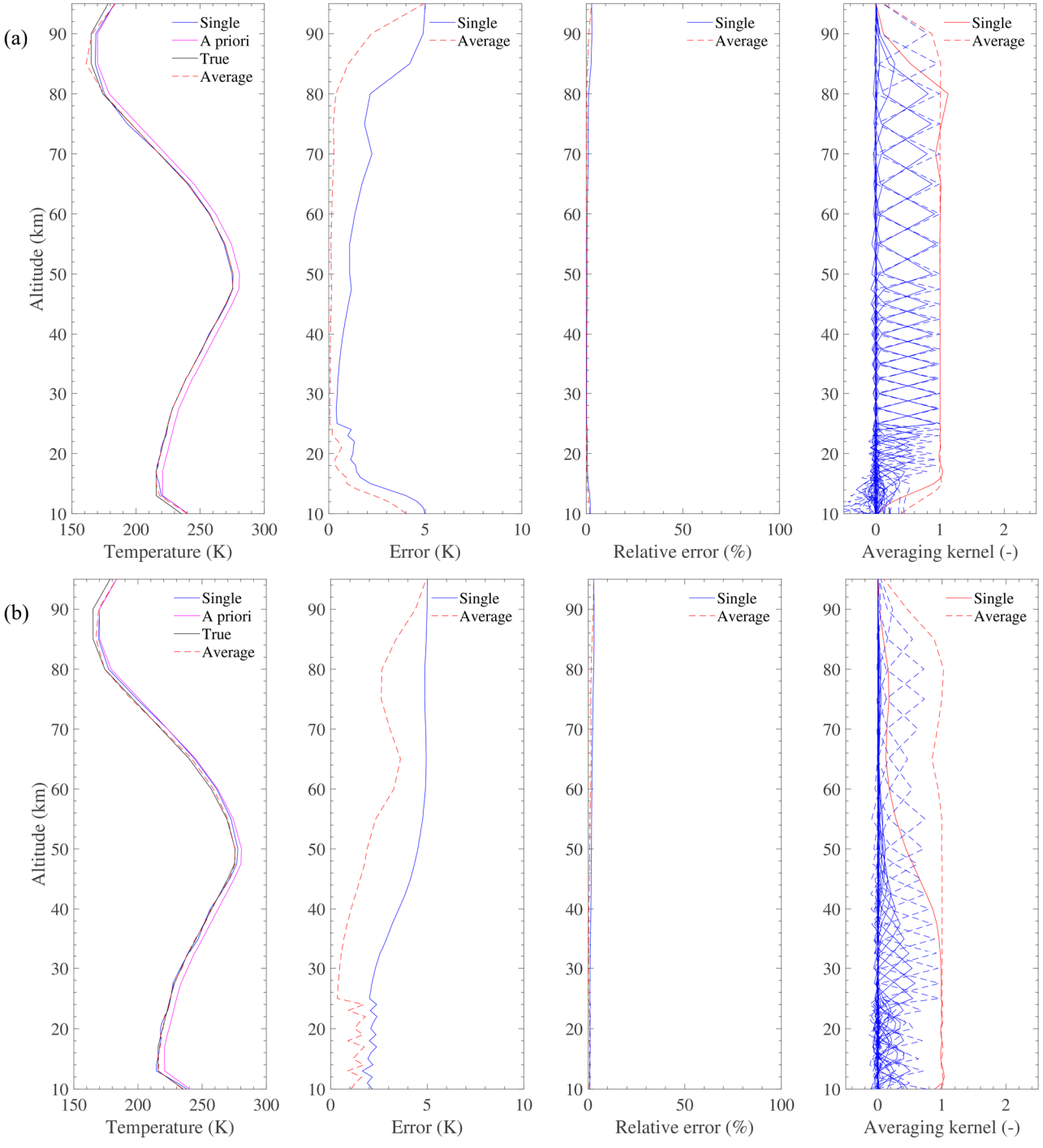

https://doi.org/10.5194/amt-2019-212
Preprint. Discussion started: 12 July 2019

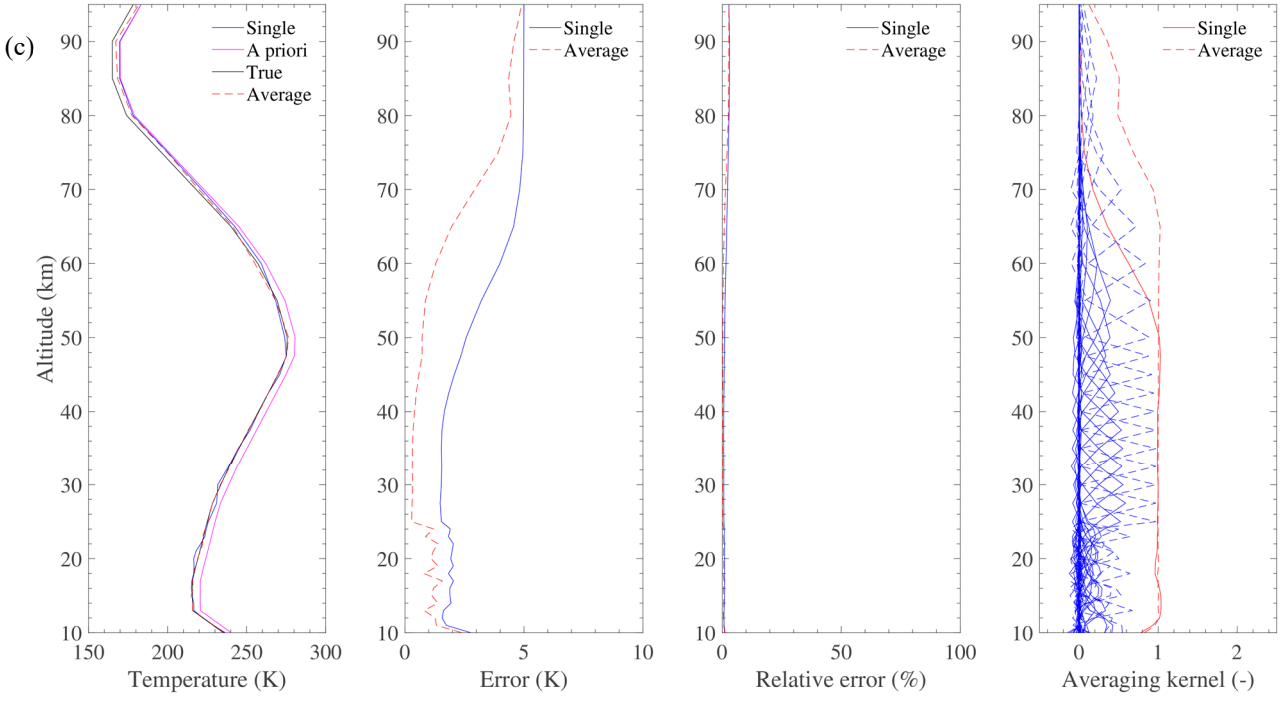

Figure 5. Simulation results of temperature retrieval using 118.75 (a), 233.95 (b), and 627.75 GHz (c) lines.

The H_2O profile is also a widely concerned parameter can be measured by 190 and 643 GHz radiometers. The 183.31 GHz line is generally used by humidity sounder to detect water vapour with high precision. Figure 6 shows the retrieval precisions for H_2O. Precision will be < 10% from 25 to 75 km by 190 GHz single scan measurement. Averaged measurement has the retrieval precision of ~ 1% at 25–80 km, < 20% at other effective altitudes. However, the precision of 643 GHz radiometer is much worse than that of 190 GHz.

https://doi.org/10.5194/amt-2019-212
Preprint. Discussion started: 12 July 2019

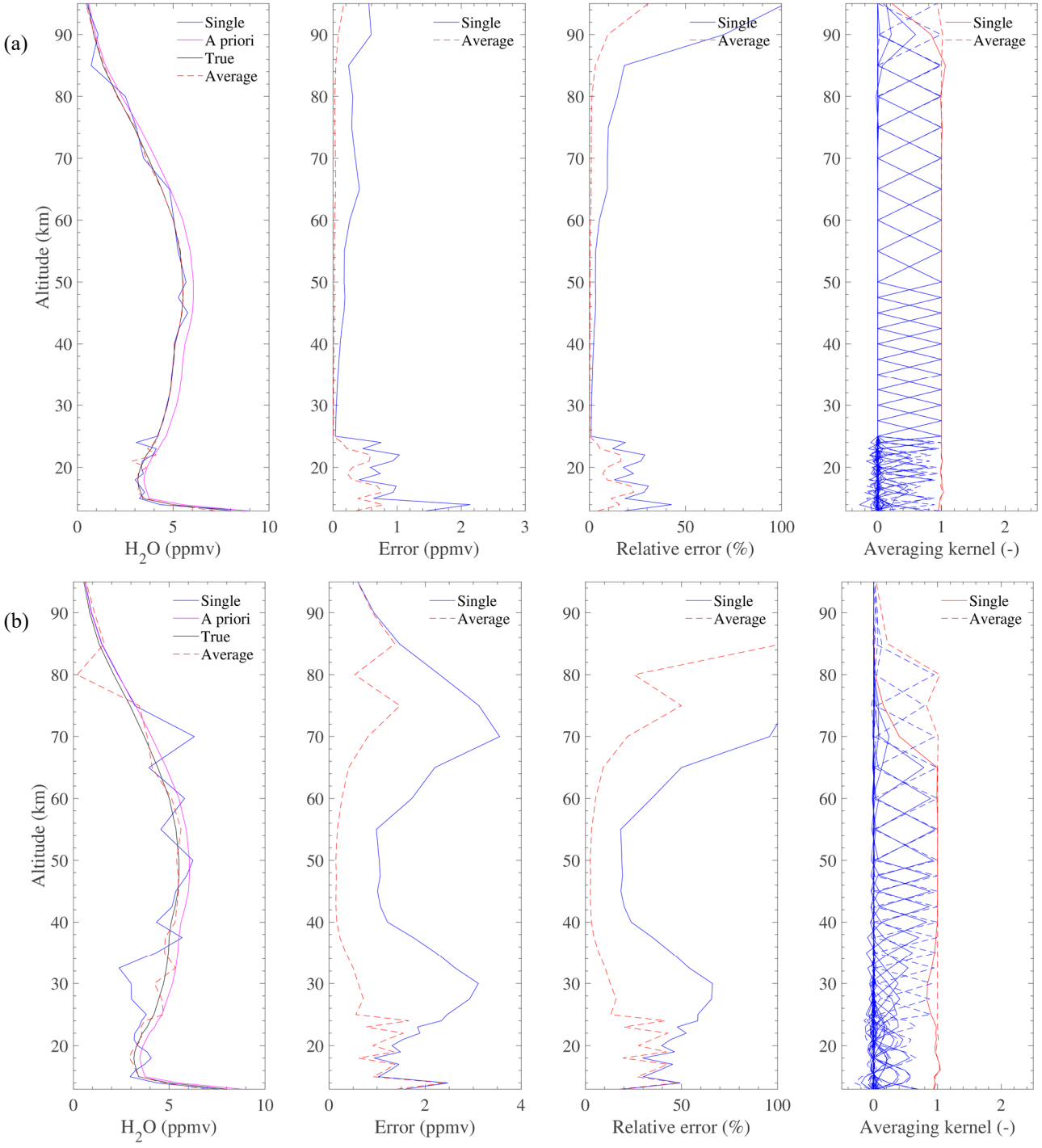

Figure 6. Simulation results of H_2O retrieval using 183.31 (a) and 657.9 GHz (b) lines.

https://doi.org/10.5194/amt-2019-212
Preprint. Discussion started: 12 July 2019

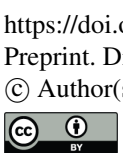

Atmospheric Measurement Techniques Discussions

O_3 has quite strong intensity in most spectral regions of TALIS. All the radiometers except 118 GHz can be used to observe this gas which is important for energy balance (Fig. 7). The 240 GHz radiometer which covering the 235.7 GHz line has the highest O_3 sensitivity. The profile can be retrieved with a single scan precision of < 5% from 25 to 55 km. By averaging the measurements, the precision will be ~ 1% at 25–60 km. The other two retrievals have relatively poor precision.

(a)

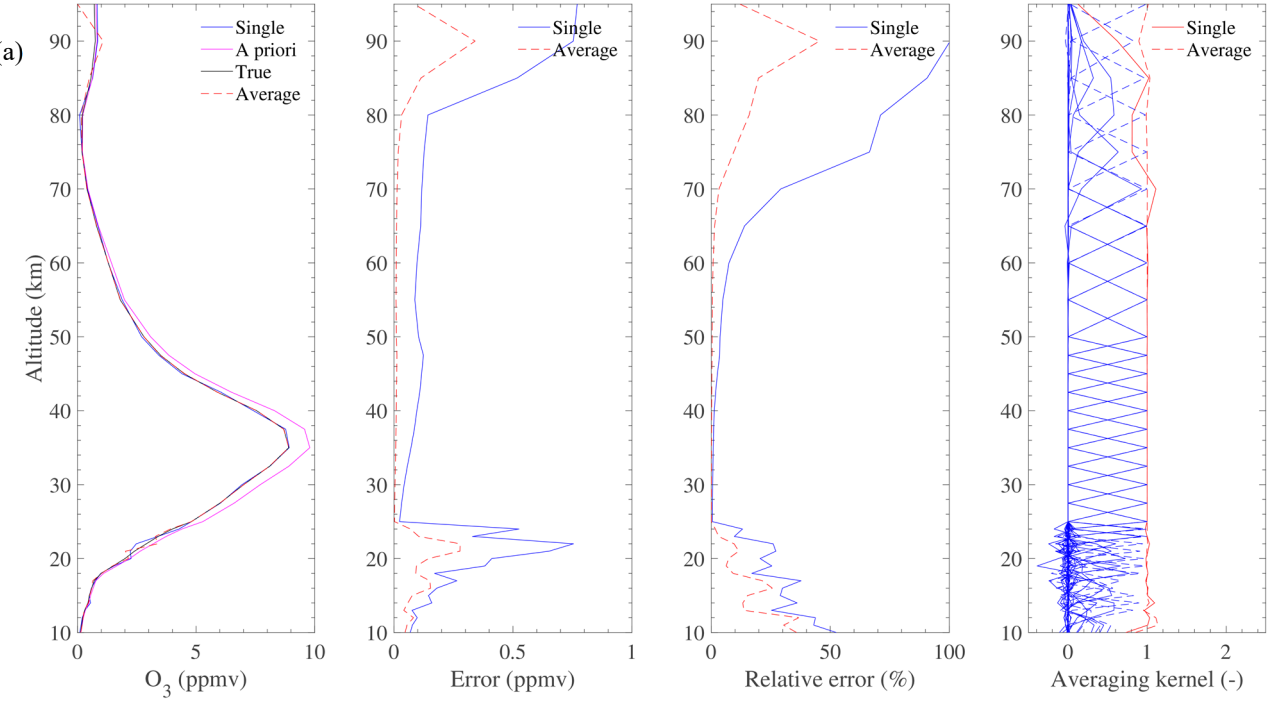

https://doi.org/10.5194/amt-2019-212
Preprint. Discussion started: 12 July 2019

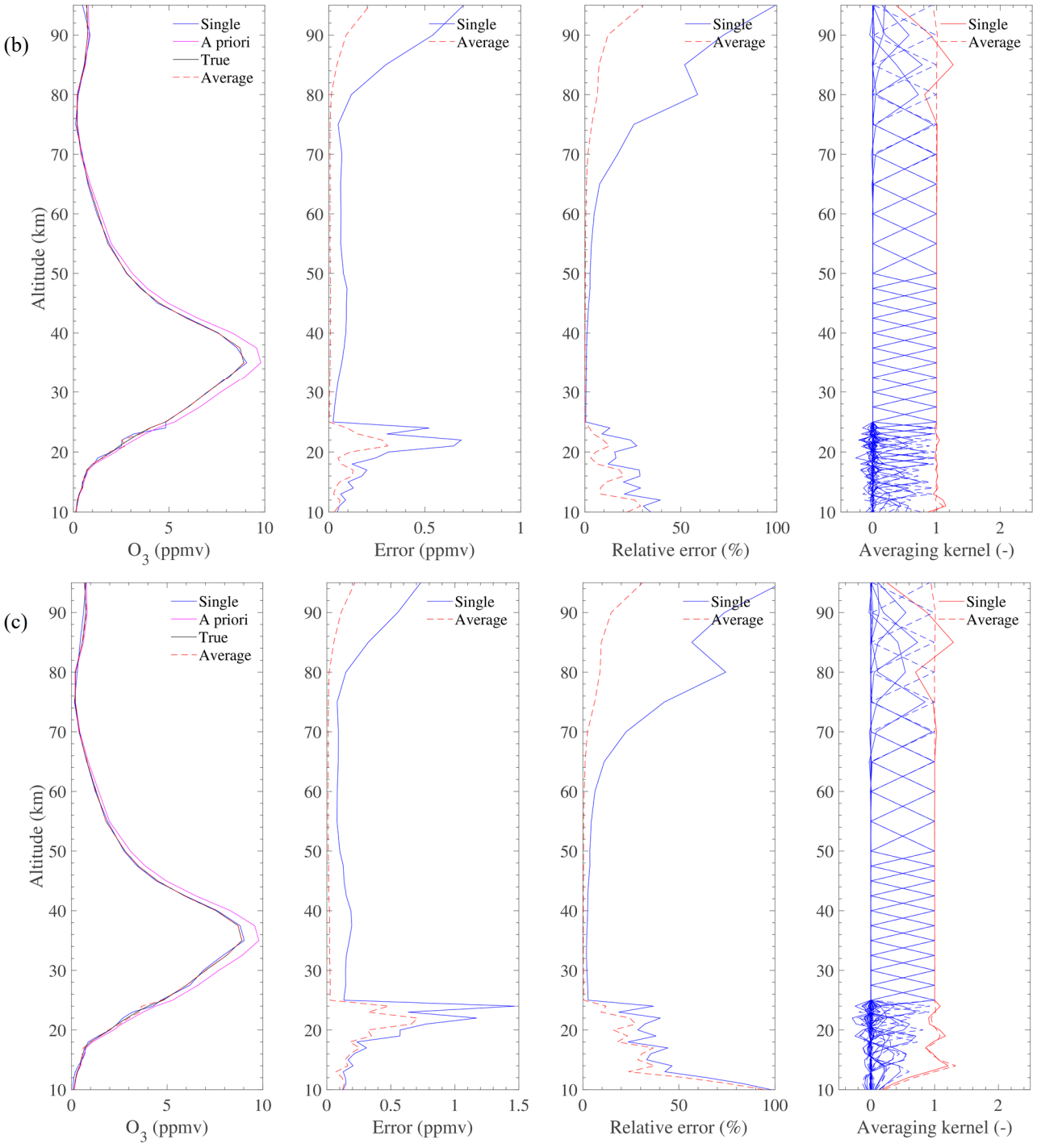

Figure 7. Simulation results of O_3 retrieval using 190 (a), 235.7 (b), and 657.5 GHz (c) lines.

https://doi.org/10.5194/amt-2019-212
Preprint. Discussion started: 12 July 2019

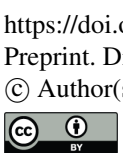

Atmospheric Measurement Techniques Discussions

HNO_3 is a common species widely exist in the stratosphere and has stable lines at 240 and 643 GHz bands. Figure 8 shows the results of HNO_3 retrievals. The 240 GHz radiometer can measure HNO_3 at 15–35 km altitude range with a good single scan relative error of 10–50%. Averaging the measurements can improve the retrieval with < 50% relative error from 10 to 45 km. The precision of 643 GHz radiometer seems bad but has some information at higher altitude.

(a)

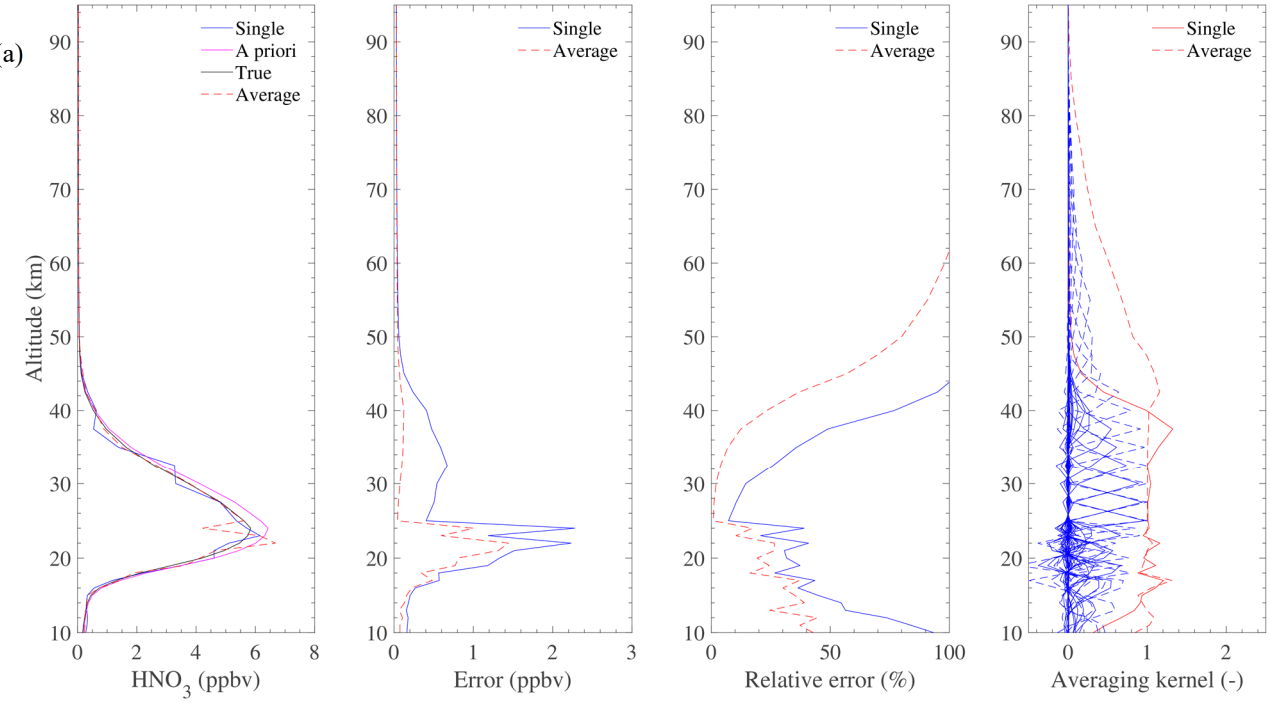

https://doi.org/10.5194/amt-2019-212
Preprint. Discussion started: 12 July 2019

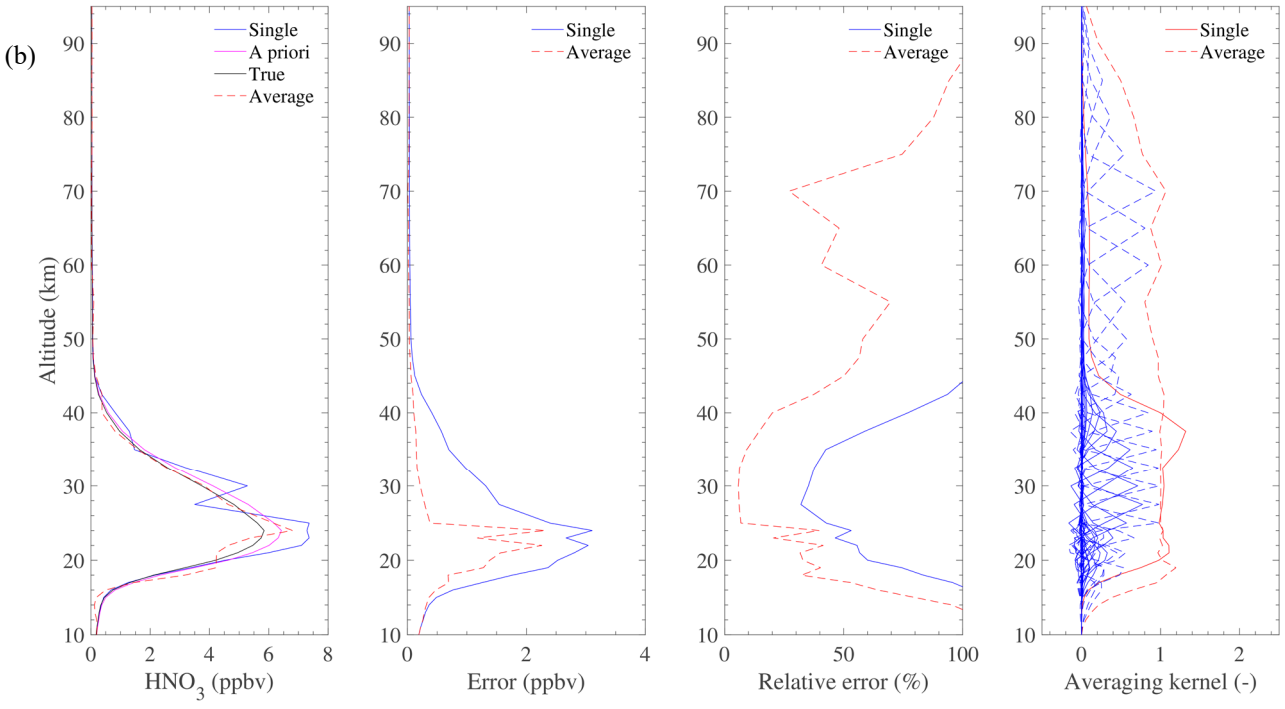

Figure 8. Simulation results of HNO_3 retrieval using 244 (a), and 656 GHz (b) lines.

Figure 9 shows the expected precision of HCl observation. HCl can be measured at 15–70 km with 10–50% single scan relative error. By averaging the measurements, the error will be < 10% at 25–75 km, < 40% at other altitudes.

https://doi.org/10.5194/amt-2019-212
Preprint. Discussion started: 12 July 2019

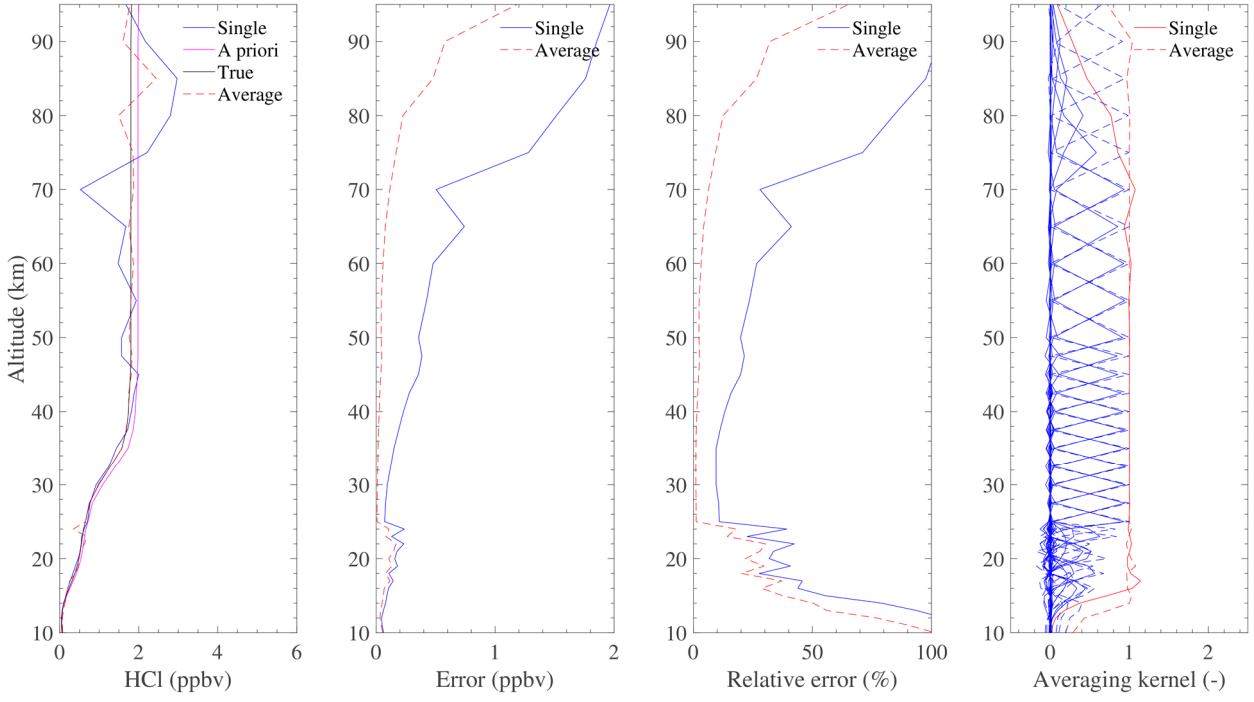

Figure 9. Simulation result of HCl retrieval using 624.9 GHz lines.

N_2O can be retrieved by 190 GHz in the upper troposphere while 643 GHz can provide more information in the stratosphere. Figure 10 shows that single scan precision of 190 GHz is about 20–40% at 10–35 km. By averaging the measurements, the precision will be < 40% from 10 to 45 km. The 643 GHz can give the similar precision at 15–50 km.

https://doi.org/10.5194/amt-2019-212
Preprint. Discussion started: 12 July 2019

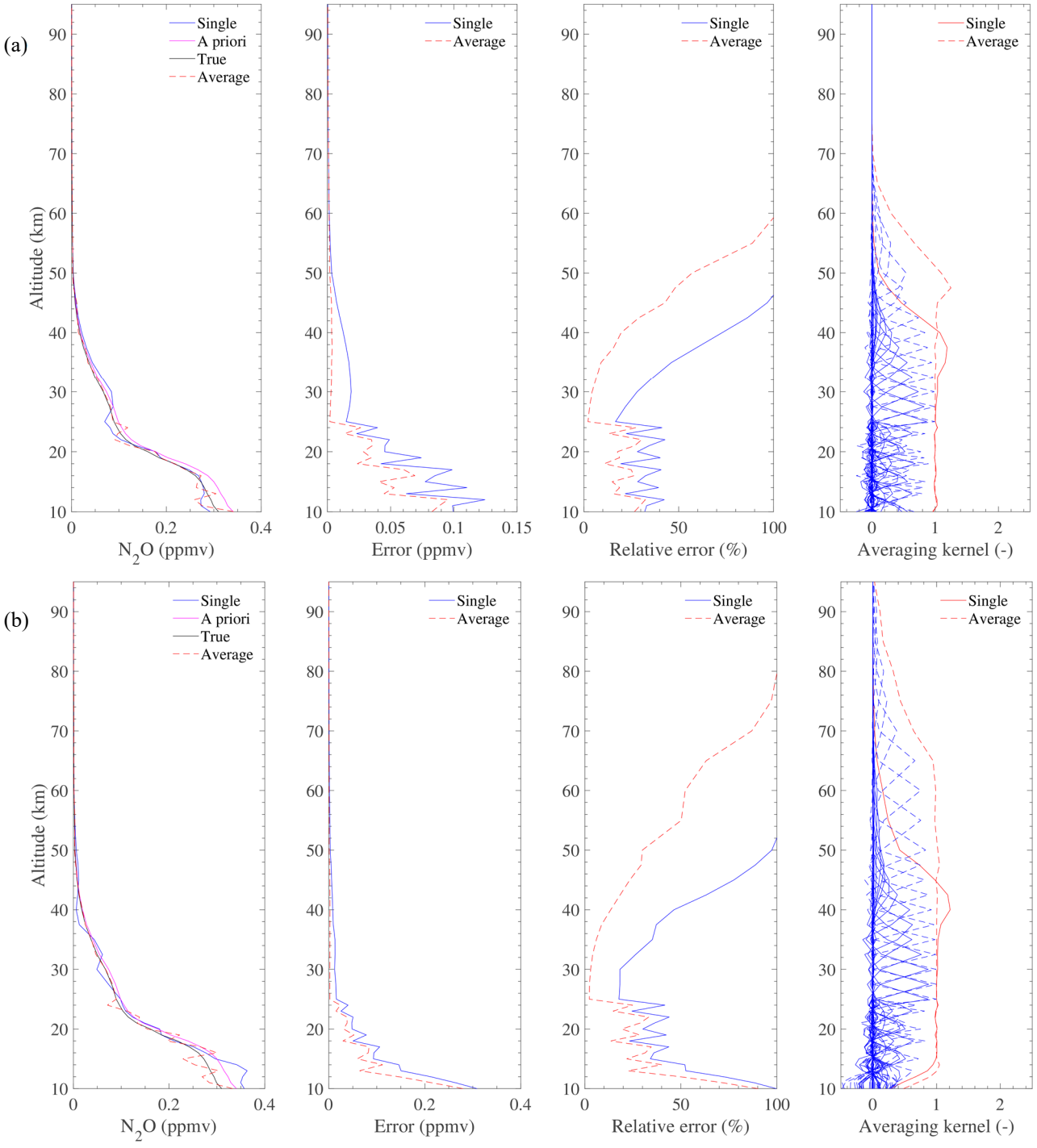

Figure 10. Simulation results of N_2O retrieval using 200.98 (a), and 652.834 GHz (b) lines.

https://doi.org/10.5194/amt-2019-212
Preprint. Discussion started: 12 July 2019

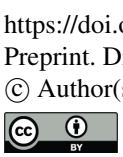

Atmospheric Measurement Techniques Discussions

ClO can be retrieved from radiances measured by 190 and 643 GHz bands (Fig. 11). However, the result shows that the 190 GHz band is not desirable for ClO observation compared with 643 GHz band. Single scan measurement from 643 GHz radiometer can be used to obtain ClO with 30–50% precision from 30 to 45 km. By averaging the measurements, precision will be 5–30% from 25 to 60 km.

(a)

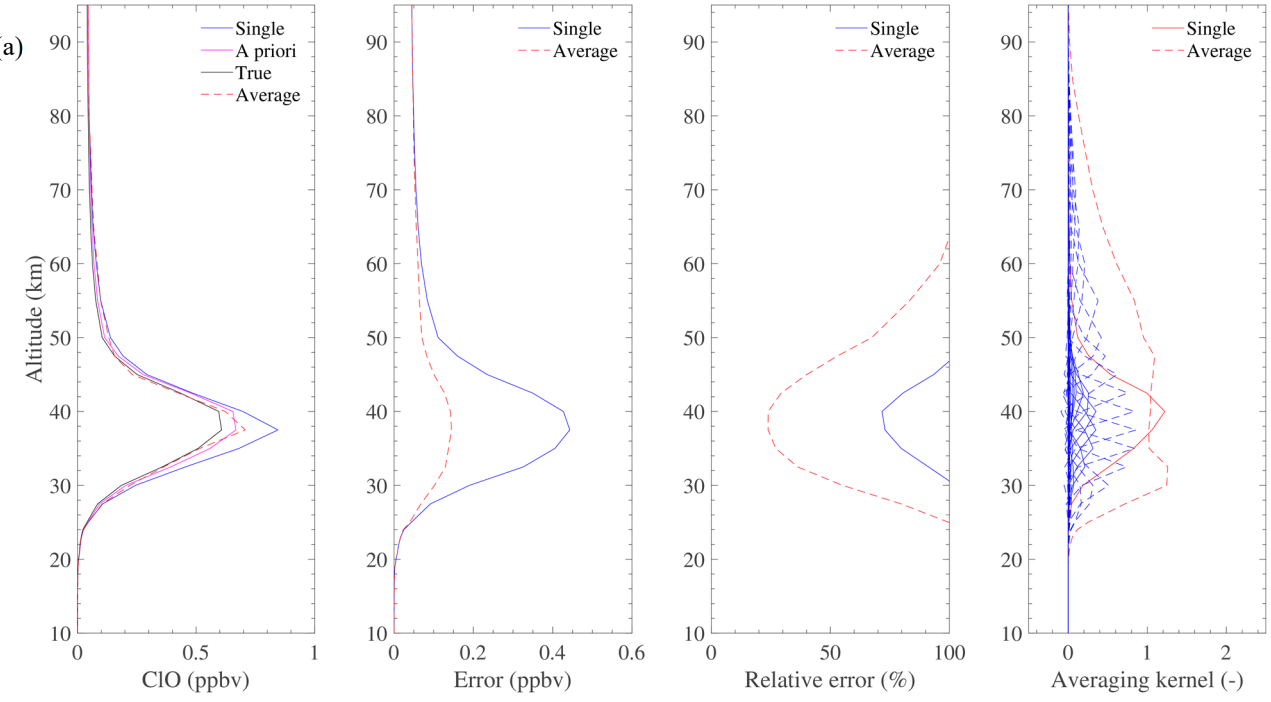

https://doi.org/10.5194/amt-2019-212
Preprint. Discussion started: 12 July 2019

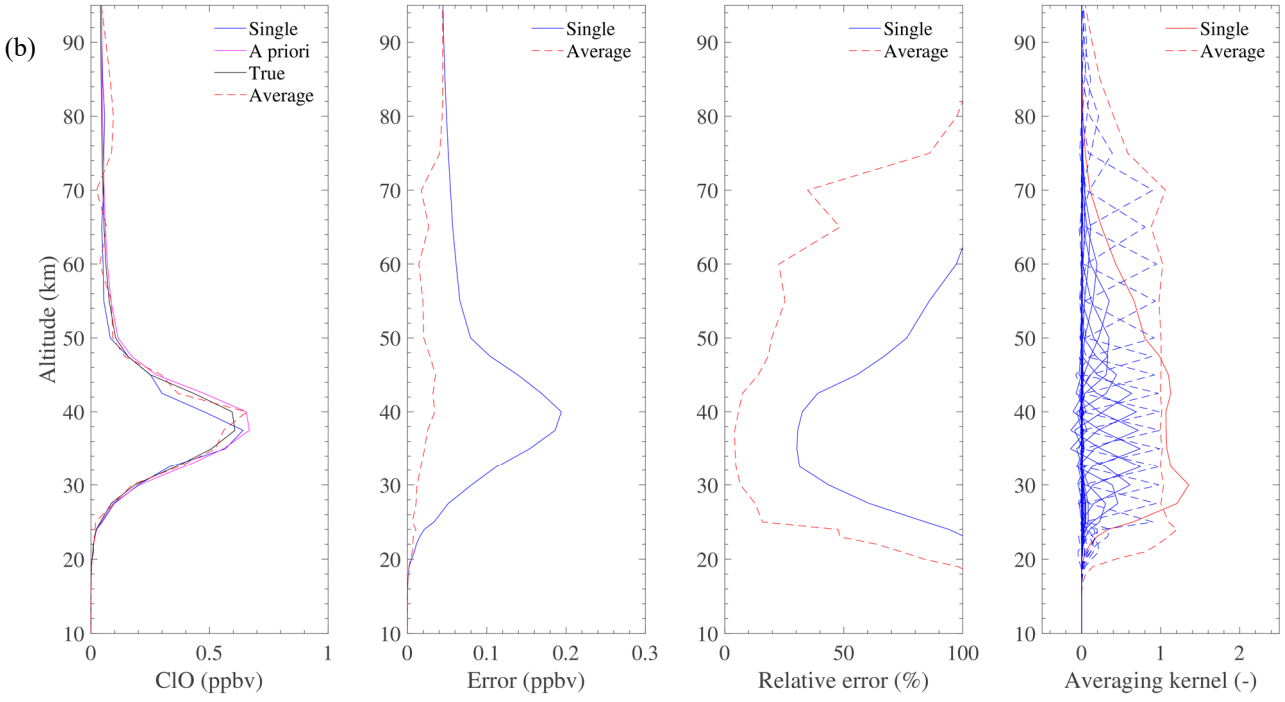

Figure 11. Simulation results of ClO retrieval using 203.4 (a) and 649.45 GHz (b) lines.

4.2.2 Medium precision products

Medium precision products including CO, HCN, CH_3Cl mean that their single scan retrieval precisions are not satisfying, but can be used to some degree. There is a choice for the user to select the single scan or averaged products.

CO can be measured using 230.538 and 661.07 GHz lines. Figure 12 shows that the 240 GHz radiometer can provide CO information with 40–90% single scan precision from 10 to 70 km. By using averaged measurements, CO can be retrieved with < 40% relative error from 10 to 25 km, < 20% relative error at the range of 25–95 km. However, the retrieval of 643 GHz measurement shows poor precision.

https://doi.org/10.5194/amt-2019-212
Preprint. Discussion started: 12 July 2019

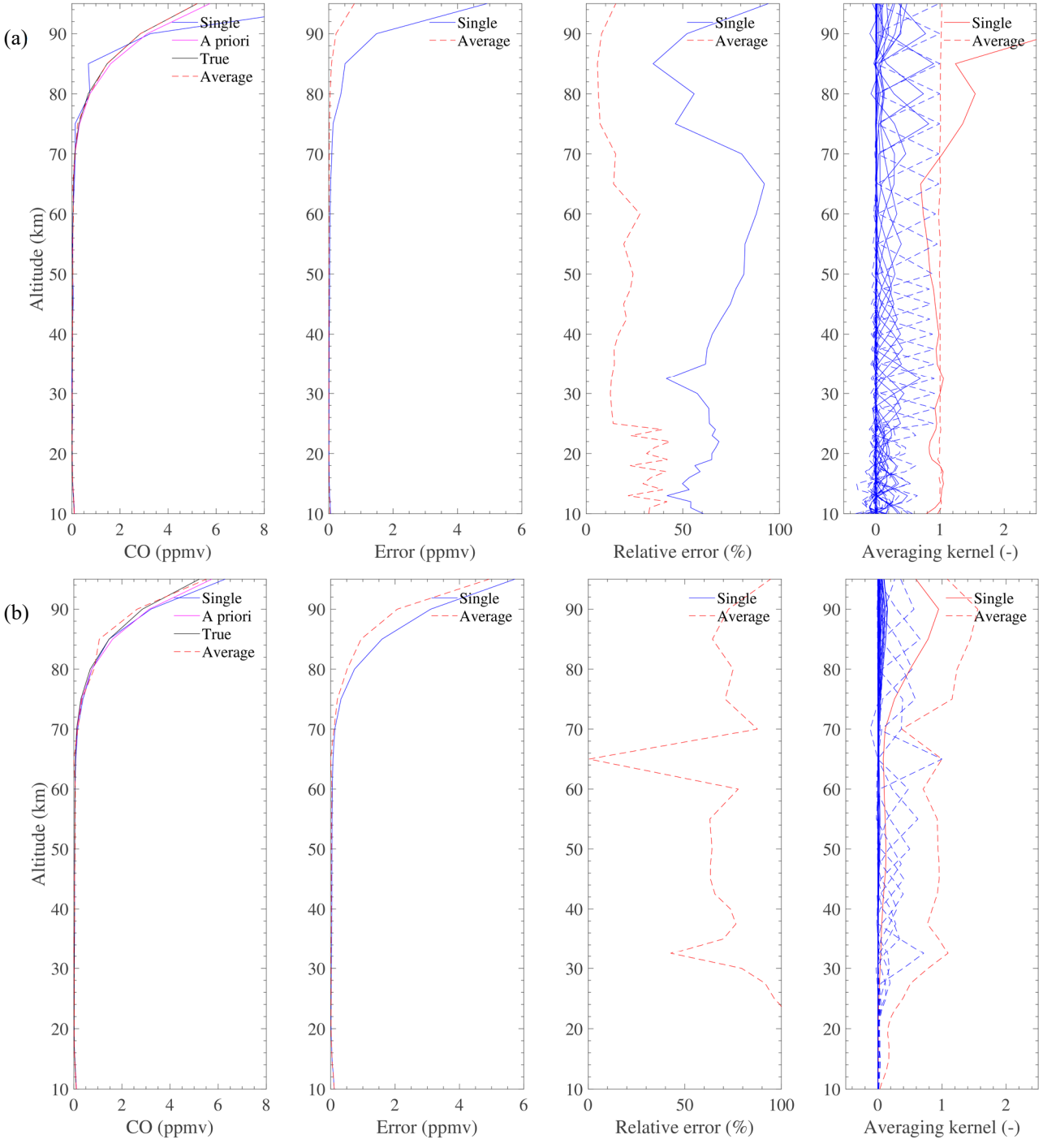

Figure 12. Simulation results of CO retrieval using 230.538 (a) and 661.07 GHz (b) lines.

https://doi.org/10.5194/amt-2019-212
Preprint. Discussion started: 12 July 2019

Atmospheric Measurement Techniques Discussions

HCN is measured by 190 GHz radiometer at 177.26 GHz line. The single scan precision is around 50% from 18 to 32 km (Fig. 13). By averaging the measurements, the relative error will be < 50% at 15–60 km.

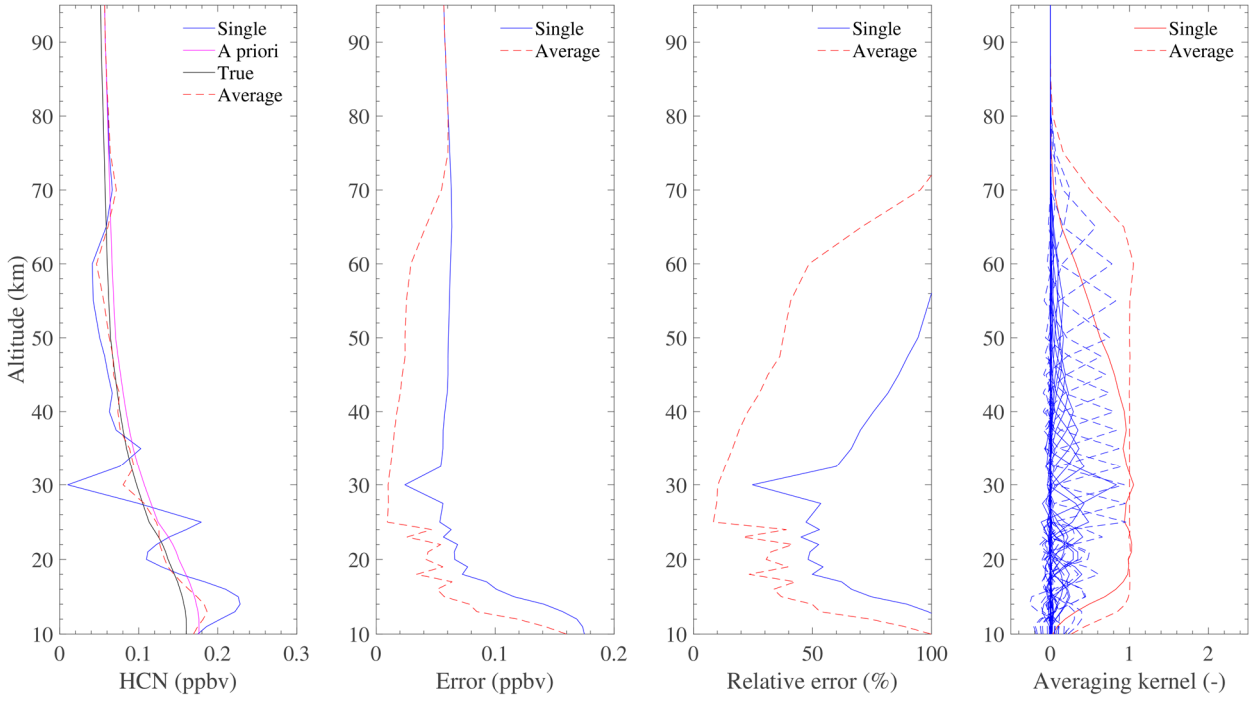

Figure 13. Simulation result of HCN retrieval using 177.26 GHz line.

CH_3Cl can be measured by the 643 GHz radiometer. As the result shows (Fig. 14), the 649.5 GHz band are suitable for CH_3Cl observation in the upper troposphere and lower stratosphere. It can be measured with 40–50% single scan precision from 15 to 23 km, with 20–50% averaged precision from 12 to 30 km.

https://doi.org/10.5194/amt-2019-212
Preprint. Discussion started: 12 July 2019

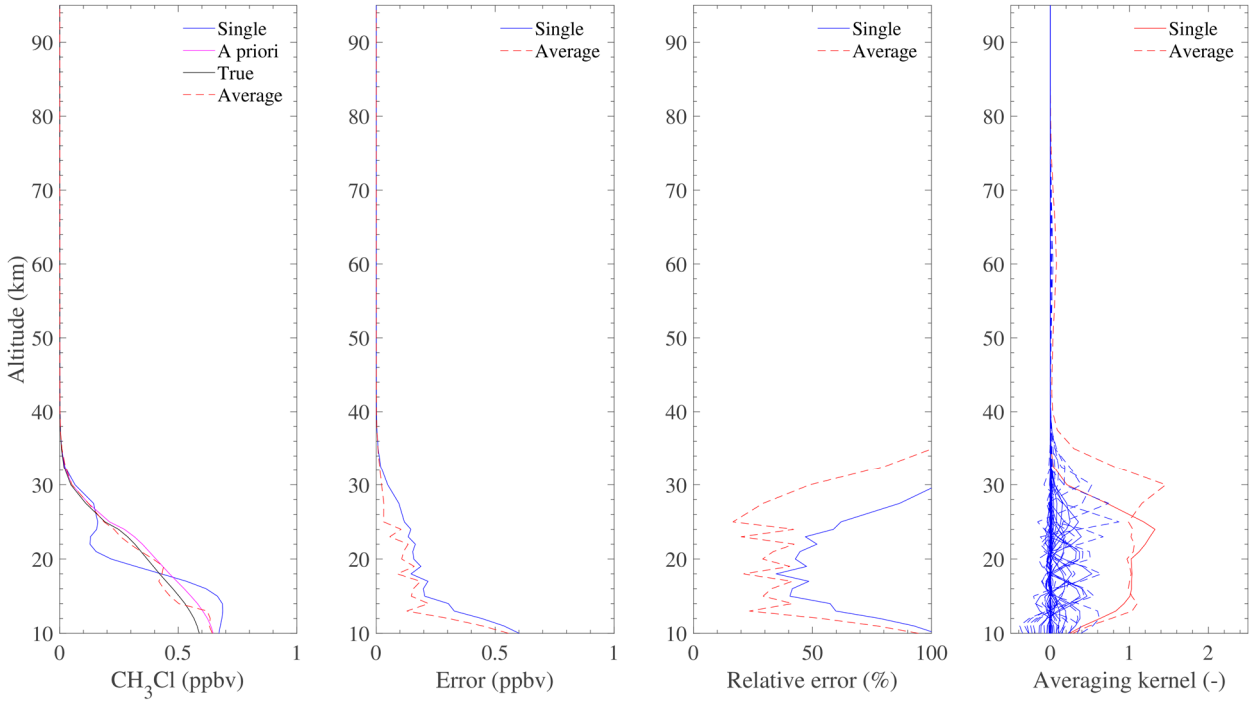

Figure 14. Simulation results of CH_3Cl retrieval using 649.5 GHz lines.

4.2.3 Low precision products

There are several weak lines exist in the spectral regions of TALIS such as HOCl, BrO, and HO_2. Significantly average must be done to these measurements in order to obtain reliable and satisfying precision.

The 635.87 GHz line is the most appropriate line for HOCl observation. However, the single scan retrieval has poor precision of 70–100%. Figure 15 reveals that HOCl can be retrieved from 22 to 52 km with averaged measurement precision of 15–50%.

https://doi.org/10.5194/amt-2019-212
Preprint. Discussion started: 12 July 2019

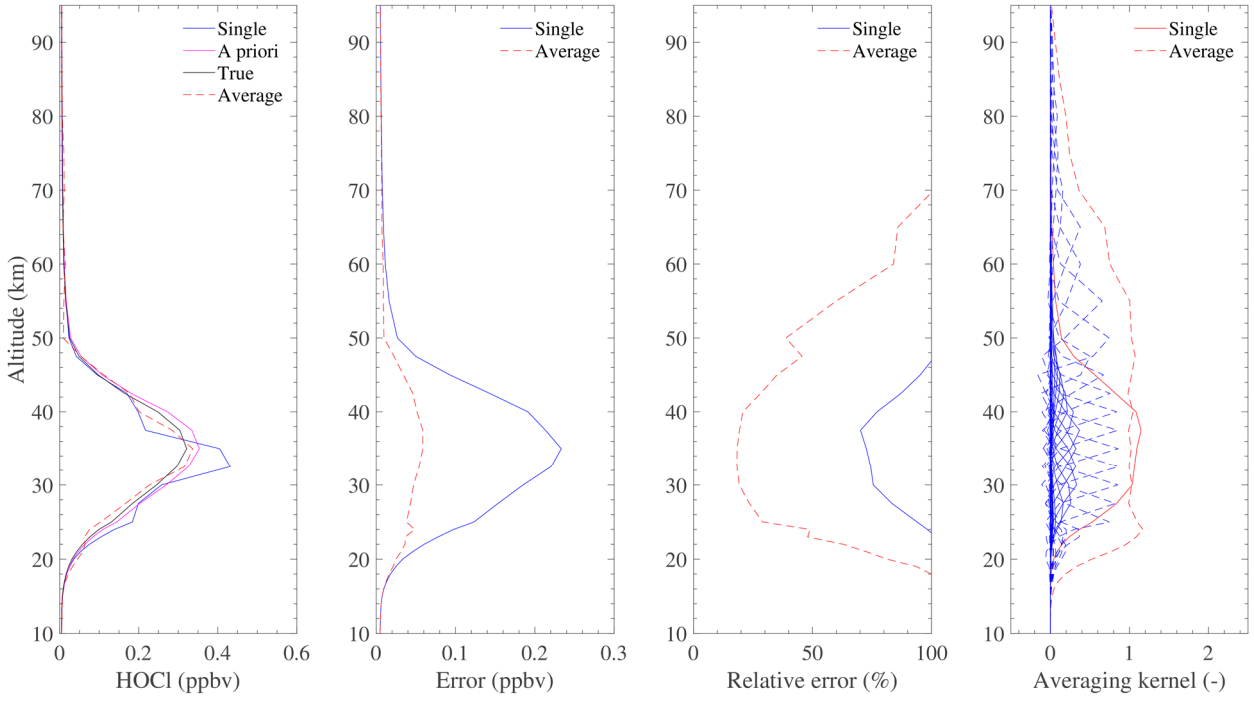

Figure 15. Simulation result of HOCl retrieval using 635.87 GHz line.

BrO can be measured by using 624.768 GHz spectral line. Figure 16 shows the simulation result of BrO retrieval. As the averaging kernel reveals, there is almost no useful information in single scan measurement because of the quite poor signal-to-noise ratio. Therefore, averaging is needed to obtain reliable and scientific results. The error is 50–80% from 23 to 56 km.

https://doi.org/10.5194/amt-2019-212
Preprint. Discussion started: 12 July 2019

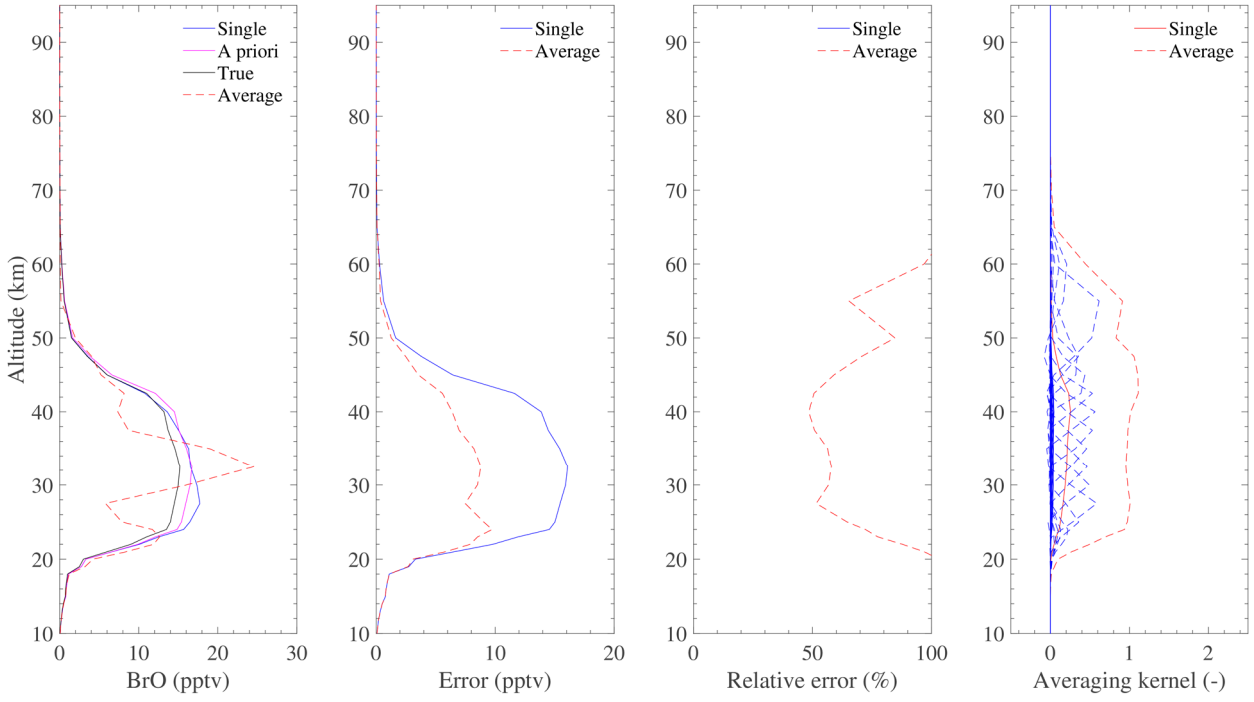

Figure 16. Simulation results of BrO retrieval using 624.768 GHz line.

HO_2 can be measured by the 643 GHz radiometer with 10–50% relative error at the vertical range of 35–85 km by using averaged data (Fig. 17). The precision of single scan retrieval is not desirable because of the weak signal.

https://doi.org/10.5194/amt-2019-212
Preprint. Discussion started: 12 July 2019

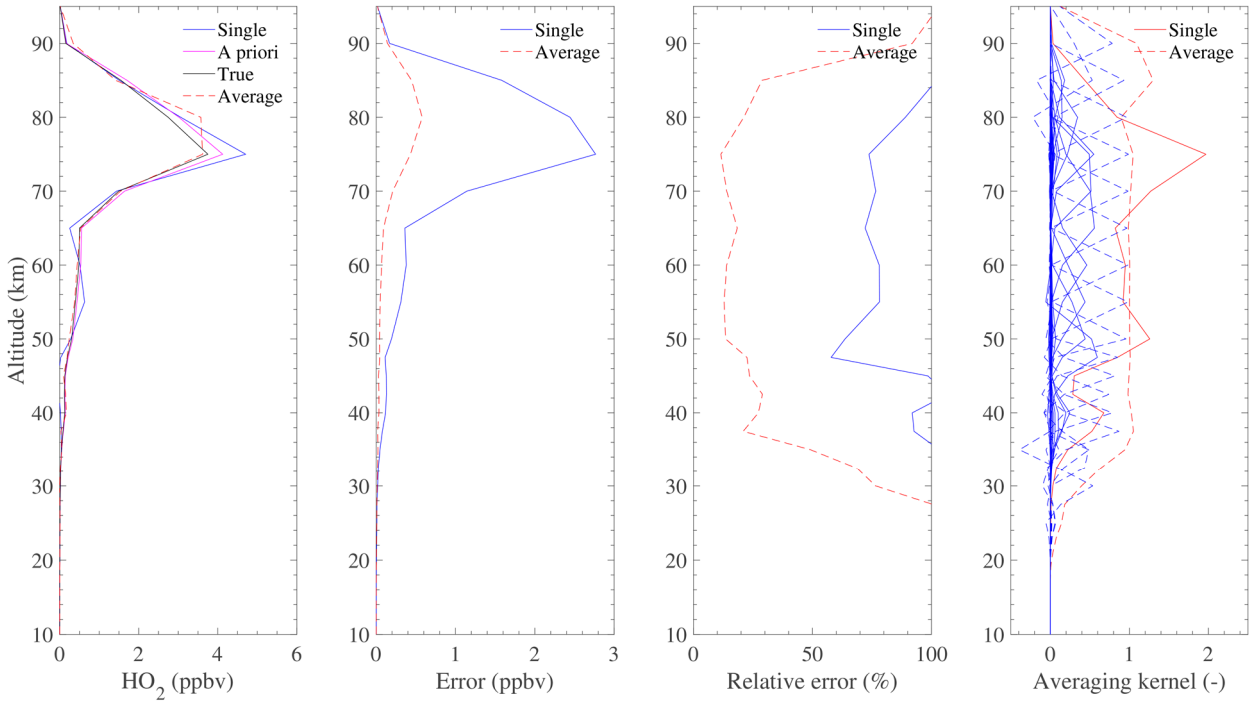

Figure 17. Simulation results of HO_2 retrieval using 649.701 GHz line.

4.2.4 Promising products

The unique products are the target species which are not covered by EOS MLS but covered by TALIS. There are four gases: NO, NO_2, H_2CO, and SO_2. However, their signals all have weak intensity and must be averaged to improve the retrieval precision.

NO can be retrieved from averaged data with 10–40% precision at 30–95 km (Fig. 18). While its single scan measurement has no information in the area where NO mainly exists.

https://doi.org/10.5194/amt-2019-212
Preprint. Discussion started: 12 July 2019

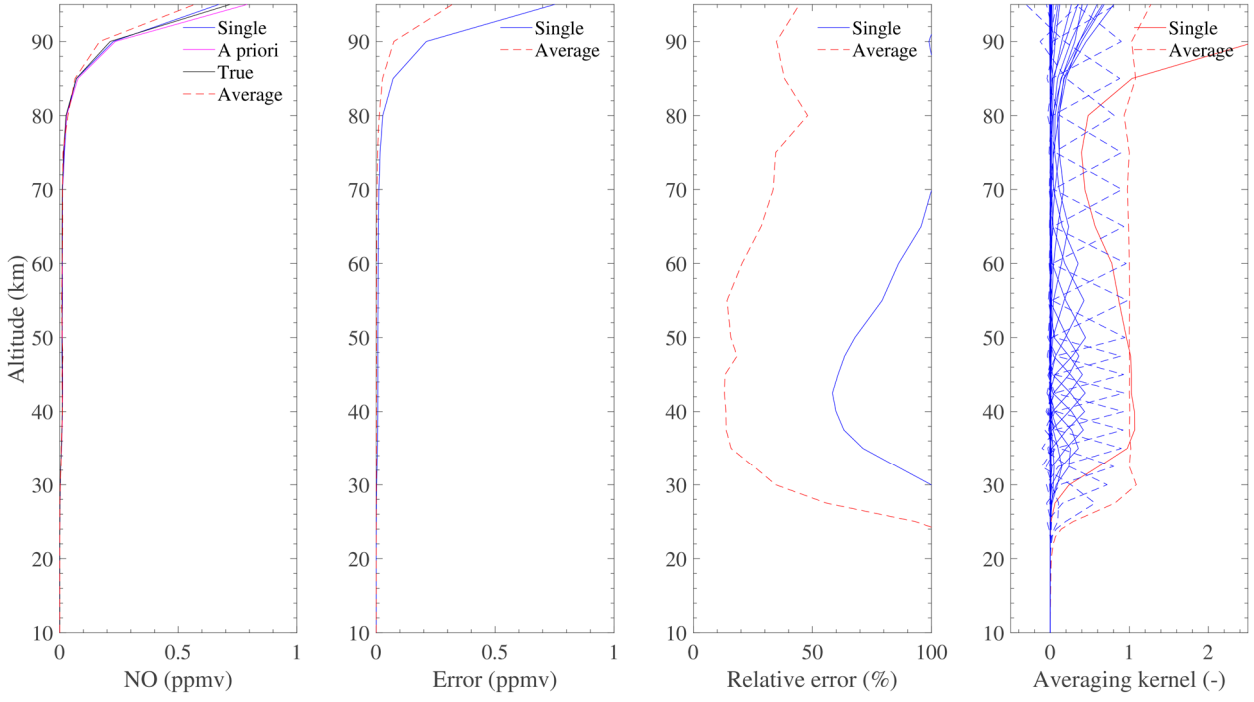

Figure 18. Simulation result of NO retrieval using 651.75 GHz line.

NO_2 has a weak line in the spectrum of 240 GHz band. Figure 19 shows that only averaged measurement can provide some information at 25–40 km with the precision of about 50%.

https://doi.org/10.5194/amt-2019-212
Preprint. Discussion started: 12 July 2019

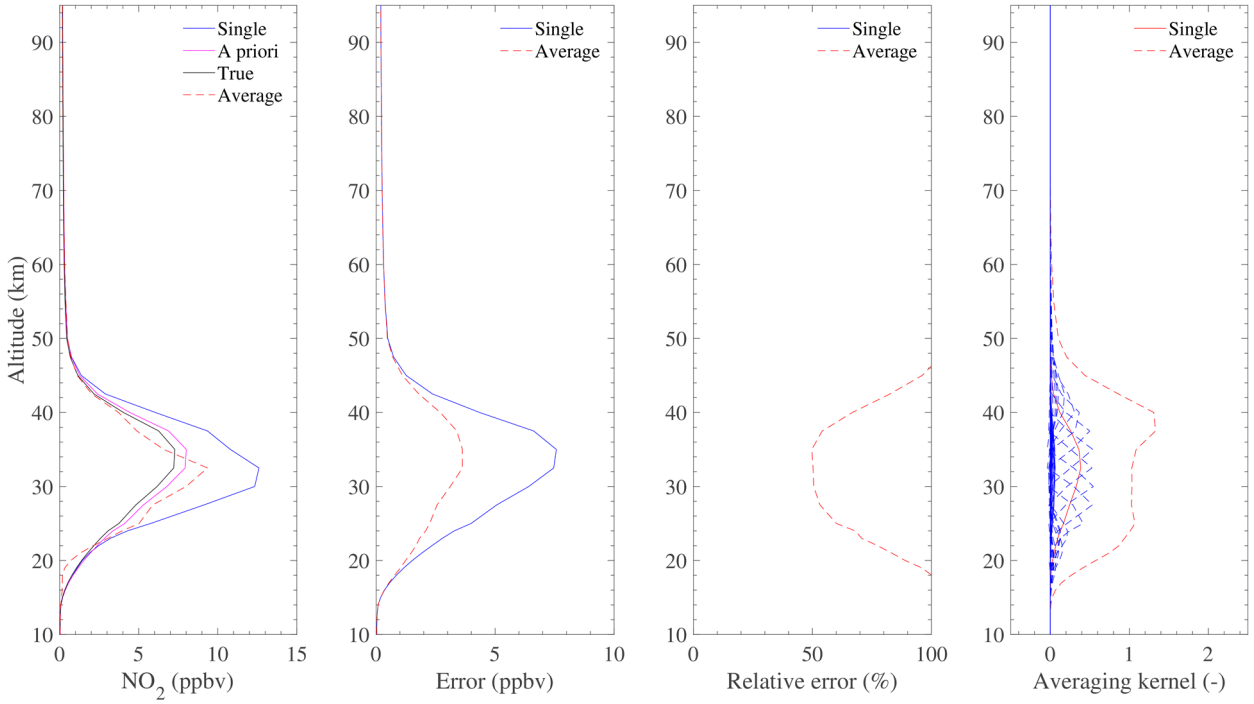

Figure 19. Simulation result of NO_2 retrieval using 232.7 GHz lines.

Although H_2CO has a line at 656.45 GHz, its emission radiance is too weak. Almost no useful information can be obtained (Fig. 20). However, this line has the potential to measure H_2CO. More average or other effective methods should be applied to get acceptable precision.

https://doi.org/10.5194/amt-2019-212
Preprint. Discussion started: 12 July 2019

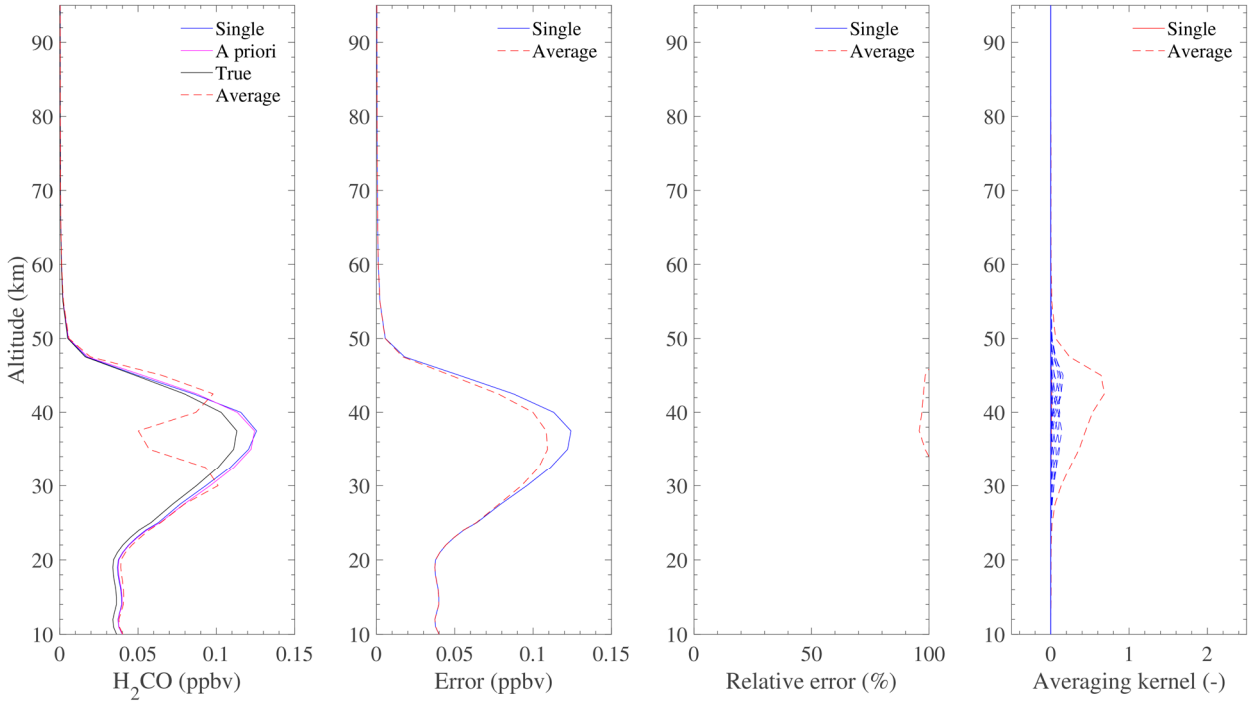

Figure 20. Simulation result of H_2CO retrieval using 656.45 GHz line.

MLS standard SO_2 product is taken from the 240 GHz retrieval, but only effective when its concentration significantly enhanced. TALIS has both 240 and 643 GHz radiometer which covering the lines of SO_2. The 240 GHz radiometer can be used to measure SO_2 like the way of MLS. The 643 GHz radiometer can give the concentration of nominal background. The averaged result shows that SO_2 can be retrieved at 40–75 km with the relative error about 20–60% (Fig. 21).

https://doi.org/10.5194/amt-2019-212
Preprint. Discussion started: 12 July 2019

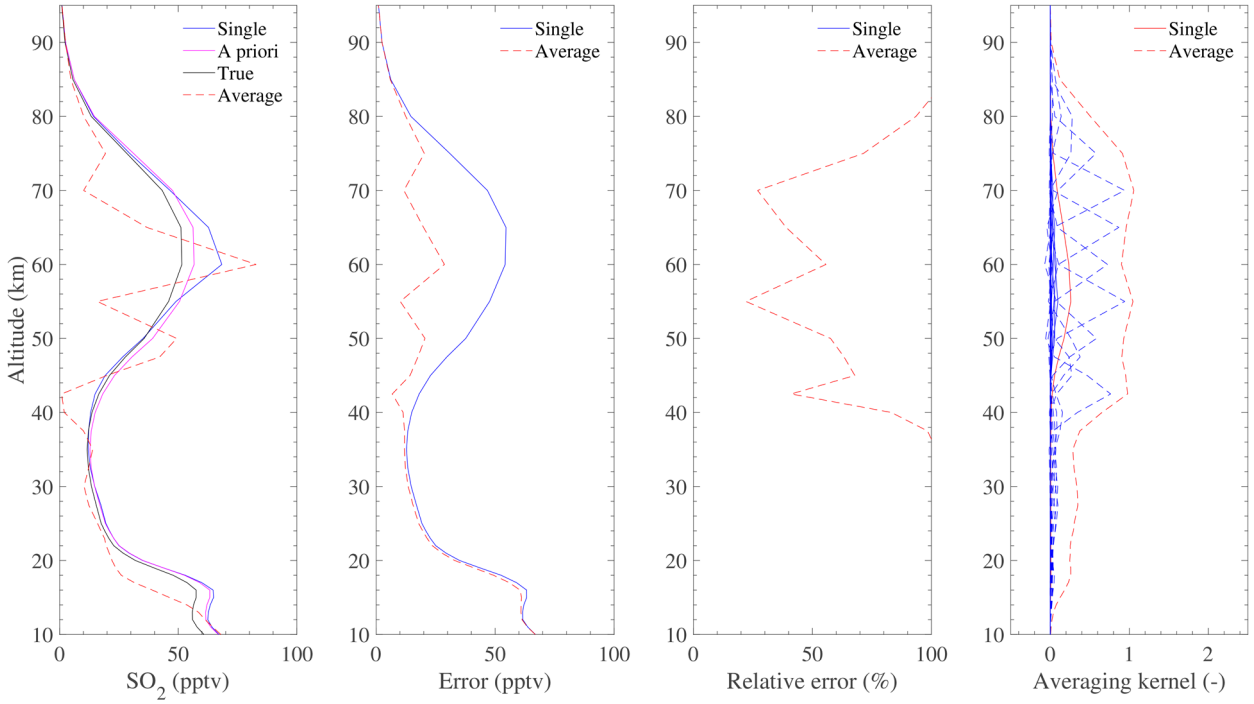

Figure 21. Simulation result of SO_2 retrieval using 659 GHz lines.

5 Conclusions

Simulation analysis for temperature and chemical species retrieval have been performed to assess the measurement performance of TALIS and to support the mission. This study mainly focuses on a large number of important chemical species in middle and upper atmosphere which can be observed by limb sounder. The results are summarized in Table 2.

The results of seven high sensitivity products are reliable. 118, 240, and 643 GHz observations of O_2 are used to estimate temperature profile which is quite important in meteorology. The 118 GHz radiometer can obtain temperature < 2 K precision at 15–80 km and the 240 GHz radiometers can provide the information in the upper troposphere. 190 GHz radiometer can be used to measure H_2O < 10% precision in a wide vertical range and give information of upper tropospheric humidity. O_3 can be measured by three radiometers and the 240 GHz has the best precision. It can be < 5% from 25 to 60 km by single scan measurement. HNO_3 can be derived from 240 GHz retrieval with good precision of < 40%. The result of HCl single scan retrieval which < 40% in most atmospheric area is quite acceptable. The 190 GHz radiometer can give a good estimate to N_2O profile with 20–40% relative error, while 643 GHz measurement can provide information at higher altitudes. Single scan precision of ClO measured by 643 GHz radiometer is enough in the area where ClO mainly exists. CH_3Cl can be measured in the upper troposphere and low stratosphere with about 50% precision. The profile of CO retrieved from 240 GHz measurement is better than that from 643 GHz measurement. Although the single scan precision seems not very good,

https://doi.org/10.5194/amt-2019-212
Preprint. Discussion started: 12 July 2019

Atmospheric Measurement Techniques Discussions

it is acceptable at 70–90 km where species mainly exist. HCN have 50% single scan precision at 18–32 km which may need to be averaged. Other measurements such as HO_2, HOCl, NO, NO_2, BrO, SO_2, and H_2CO must be significantly averaged before scientific use because of the weak signals. Apart from these target species, some potential targets are not discussed here such as cloud ice water content, cloud ice water path, CH_3OH, and CH_3CN.

TALIS has strong potential to monitor chemical composition in the whole Earth's atmosphere which is important for numerical weather prediction models and to characterize the long-time change of climate. Measurement data can be used for atmospheric chemistry and dynamics study which is quite important for the geoscience. A better understanding of the key chemical and dynamical processes in the middle and upper atmosphere will help us solve the climate problem more efficient.

This paper is the preliminary analysis of the instrument. According to this simulation, the instrument will be further optimized. In addition, more studies such as structure optimization, calibration research, and error analysis will be performed to support the mission.

Table 2. Simulation results of TALIS retrieval precision

Product	Radiometer	Single precision	Average precision
Temperature	118 GHz+240 GHz	< 2K (10–75 km)	< 1K (10–85 km)
H_2O	190 GHz	< 10% (25–75 km)	~ 1% (25–80 km)
O_3	240 GHz	< 5% (25–55 km)	~ 1% (25–70 km)
HCl	643 GHz	10–50% (15–70 km)	< 10% (25–75 km)
N_2O	190 GHz+643 GHz	20–40% (10–40 km)	< 40% (10–50 km)
HNO_3	240 GHz	10–50% (15–35 km)	< 50% (10–45 km)
ClO	643 GHz	30–50% (30–45 km)	< 30% (25–60 km)
CO	240 GHz	40–90% (10–70 km)	< 40% (10–95 km)
HCN	190 GHz	20–50% (18–32 km)	10–50% (15–60 km)
CH_3Cl	643 GHz	40–50% (15–23 km)	20–50% (12–30 km)
HOCl	643 GHz	70–90% (27–43 km)	15–50% (22–52 km)
BrO	643 GHz	/	50–80% (23–56 km)
HO_2	643 GHz	60–80% (47–67 km)	10–50% (35–85 km)
NO	643 GHz	60–80% (33–55 km)	10–40% (30–95 km)
NO_2	240 GHz	/	50–60% (25–40 km)
H_2CO	643 GHz	/	/
SO_2	643 GHz	/	20–60% (40–75 km)

https://doi.org/10.5194/amt-2019-212
Preprint. Discussion started: 12 July 2019

Atmospheric Measurement Techniques Discussions

Code and data availability. ARTS can be downloaded at http://www.radiativetransfer.org/getarts/. Qpack is included in the Atmlab which can be downloaded from http://www.radiativetransfer.org/tools/. Profiles and spectroscopy data of Perrin and HITRAN are included in ARTS XML Data. JPL molecular spectroscopy catalogue is available at https://spec.jpl.nasa.gov/. MLS version 4.2 data can be obtained at https://doi.org/10.5067/Aura/MLS/DATA3020.

Author contribution. Zhenzhan Wang designed the mission concept. Wenyu Wang performed the simulate and wrote the manuscript. Wenyu Wang and Yongqiang Duan analysed the results. Zhenzhan Wang edited the article.

Competing interests. The authors declare that they have no conflict of interest.

Acknowledgements. The authors would like to thank the ARTS and Qpack development teams for assistance configuring and running the model. The authors thank the JPL for providing spectroscopy data and MLS data. They would also like to thank the reviewers and the editors for their valuable and helpful suggestions.

References

Baron, P., Ricaud, P., de La No¨e, J., Eriksson, P., Merino, F., Ridal, M., and Murtagh, D. P.: Studies for the Odin Sub-Millimetre Radiometer. II. Retrieval methodology, Can. J. Phys., 80, 341–356, https://doi.org/10.1139/P01-150, 2002.

Baron, P., Urban, J., Sagawa, H., Möller, J., Murtagh, D. P., Mendrok, J., Dupuy, E., Sato, T. O., Ochiai, S., Suzuki, K., Manabe, T., Nishibori, T., Kikuchi, K., Sato, R., Takayanagi, M., Murayama, Y., Shiotani, M., and Kasai, Y.: The Level 2 research product algorithms for the Superconducting Submillimeter-Wave Limb-Emission Sounder (SMILES), Atmos. Meas. Tech., 4, 2105-2124, https://doi.org/10.5194/amt-4-2105-2011, 2011.

Baron, P., Murtagh, D., Eriksson, P., Mendrok, J., Ochiai, S., Pérot, K., Sagawa, H., and Suzuki, M.: Simulation study for the Stratospheric Inferred Winds (SIW) sub-millimeter limb sounder, Atmos. Meas. Tech., 11, 4545-4566, https://doi.org/10.5194/amt-11-4545-2018, 2018.

Bremer, J. C.: Improvement of Scanning Radiometer Performance by Digital Reference Averaging, IEEE. T. INSTRUM. MEAS., 28, 46–54, https://10.1109/TIM.1979.4314759, 1979.

Eriksson, P., Jiménez, C., and Buehler, S. A.: Qpack, a general tool for instrument simulation and retrieval work, J. Quant. Spectrosc. Ra., 91, 47–64, https://doi.org/10.1016/j.jqsrt.2004.05.050, 2005.

Eriksson, P., Ekström, M., Melsheimer, C., and Buehler, S. A.: Efficient forward modelling by matrix representation of sensor responses, Int. J. Remote Sens., 27, 1793–1808, https://doi.org/10.1080/01431160500447254, 2006.

Eriksson, P., Ekström, M., Rydberg, B., and Murtagh, D. P.: First Odin sub-mm retrievals in the tropical upper troposphere: ice cloud properties, Atmos. Chem. Phys., 7, 471-483, https://doi.org/10.5194/acp-7-471-2007, 2007.

https://doi.org/10.5194/amt-2019-212
Preprint. Discussion started: 12 July 2019

Eriksson, P., Buehler, S. A., Davis, C. P., Emde, C., and Lemke, O.: ARTS, the atmospheric radiative transfer simulator, Version 2, J. Quant. Spectrosc. Ra., 112, 1551–1558, https://doi.org/10.1016/j.jqsrt.2011.03.001, 2011.

Johnson, D. G., Traub, W. A., Chance, K. V., Jucks, K. W., and Stachnik, R. A.: Estimating the abundance of ClO from simultaneous remote sensing measurements of HO_2, OH, and HOCl, Geophys. Res. Lett., 22, 1869–1871, https://doi.org/10.1029/95GL01249, 1995.

Kasai, Y., Sagawa, H., Kreyling, D., Dupuy, E., Baron, P., Mendrok, J., Suzuki, K., Sato, T. O., Nishibori, T., Mizobuchi, S., Kikuchi, K., Manabe, T., Ozeki, H., Sugita, T., Fujiwara, M., Irimajiri, Y., Walker, K. A., Bernath, P. F., Boone, C., Stiller, G., von Clarmann, T., Orphal, J., Urban, J., Murtagh, D., Llewellyn, E. J., Degenstein, D., Bourassa, A. E., Lloyd, N. D., Froidevaux, L., Birk, M., Wagner, G., Schreier, F., Xu, J., Vogt, P., Trautmann, T., and Yasui, M.: Validation of stratospheric and mesospheric ozone observed by SMILES from International Space Station, Atmos. Meas. Tech., 6, 2311–2338, https://doi.org/10.5194/amt-6-2311-2013, 2013.

Kikuchi, K., Nishibori, T., Ochiai, S., Ozeki, H., Irimajiri, Y., Kasai, Y., Koike, M., Manabe, T., Mizukoshi, K., Murayama, Y., Nagahama, T., Sano, T., Sato, R., Seta, M., Takahashi, C., Takayanagi, M., Masuko, H., Inatani, J., Suzuki, M., and Shiotani, M.: Overview and early results of the Superconducting Submillimeter-Wave Limb-Emission Sounder (SMILES), J. Geophys. Res.-Atmos., 115, D23306, https://doi.org/10.1029/2010JD014379, 2010.

Lambert, A., Read, W. G., Livesey, N. J., Santee, M. L., Manney, G. L., Froidevaux, L., Wu, D. L., Schwartz, M. J., Pumphrey, H. C., Jimenez, C., Nedoluha, G. E., Cofield, R. E., Cuddy, D. T., Daffer, W. H., Drouin, B. J., Fuller, R. A., Jarnot, R. F., Knosp, B. W., Pickett, H. M., Perun, V. S., Snyder, W. V., Stek, P. C., Thurstans, R. P., Wagner, P. A., Waters, J. W., Jucks, K. W., Toon, G. C., Stachnik, R. A., Bernath, P. F., Boone, C. D., Walker, K. A., Urban, J., Murtagh, D., Elkins, J. W., and Atlas, E.: Validation of the Aura Microwave Limb Sounder middle atmosphere water vapor and nitrous oxide measurements, J. Geophys. Res.-Atmos., 112, D24S36, https://doi.org/10.1029/2007JD008724, 2007.

Livesey, N. J. and Snyder, W. V.: EOS MLS Retrieval Processes Algorithm Theoretical Basis., Tech. Rep. JPL D-16159 / CL #04-2043, Jet Propulsion Laboratory, California Institute of Technology, Pasadena, California, 91109-8099, available at: https://mls.jpl.nasa.gov/data/eos_algorithm_atbd.pdf (last access: 26 March 2019), version 2.0, 2004.

Livesey, N. J., Filipiak, M. J., Froidevaux, L., Read, W. G., Lambet, A., Santee, M. L., Jiang, J. H., Pumphrey, H. C., Waters, J. W., Cofield, R. E., Cuddy, D. T., Daffer, W. H., Drouin, B. J., Fuller, R. A., Jarnot, R. F., Jiang, Y. B., Knosp, B. W., Li, Q. B., Perun, V. S., Schwartz, M. J., Snyder, W. V., Stek, P. C., Thurstans, R. P., Wagner, P. A., Avery, M., Browell, E. V., Cammas, J. P., Christensen, L. E., Diskin, G. S., Gao, R. S., Jost, H. J., Loewenstein, M., Lopez, J. D., Nedelec, P., Osterman, G. B., Sachse, G. W., and Webster, C. R.: Validation of Aura Microwave Limb Sounder O_3 and CO observations in the upper troposphere and lower stratosphere, J. Geophys. Res.-Atmos., 113, D15S02, https://doi.org/10.1029/2007JD008805, 2008.

Livesey, N. J., Logan, J. A., Santee, M. L., Waters, J. W., Doherty, R. M., Read, W. G., Froidevaux, L., and Jiang, J. H.: Interrelated variations of O_3, CO and deep convection in the tropical/subtropical upper troposphere observed by the Aura

Microwave Limb Sounder (MLS) during 2004–2011, Atmos. Chem. Phys., 13, 579-598, https://doi.org/10.5194/acp-13-579-2013, 2013.

Livesey, N. J., Read, W. G., Wagner, P. A., Froidevaux, L., Lambert, A., Manney, G. L., Millán, L. F., Pumphrey, H. C., Santee, M. L., Schwartz, M. J., Wang, S. H., Fuller, R. A., Jarnot, R. F., Knosp, B. W., Martinez, E., Lay, R. R.: Earth Observing System (EOS) Aura Microwave Limb Sounder (MLS) Version 4.2x Level 2 data quality and description document., Tech. Rep. JPL D-33509 Rev. D, Jet Propulsion Laboratory, California Institute of Technology, Pasadena, California, 91109-8099, available at: https://mls.jpl.nasa.gov/data/v4-2_data_quality_document.pdf (last access: 26 March 2019), Version 4.2x–3.1, 2018.

Marks, C. J. and Rodgers, C. D.: A retrieval method for atmospheric composition from limb emission measurements, J. Geophys. Res.-Atmos., 98, 14939–14953, https://doi.org/10.1029/93JD01195, 1993.

Mätzler, C.: Thermal Microwave Radiation: Applications for Remote Sensing, vol. 52, Iet, 2006.

Millán, L., Livesey, N., Read, W., Froidevaux, L., Kinnison, D., Harwood, R., MacKenzie, I. A., and Chipperfield, M. P.: New Aura Microwave Limb Sounder observations of BrO and implications for Br_y, Atmos. Meas. Tech., 5, 1741-1751, https://doi.org/10.5194/amt-5-1741-2012, 2012.

Millán, L., Wang, S., Livesey, N., Kinnison, D., Sagawa, H., and Kasai, Y.: Stratospheric and mesospheric HO_2 observations from the Aura Microwave Limb Sounder, Atmos. Chem. Phys., 15, 2889-2902, https://doi.org/10.5194/acp-15-2889-2015, 2015.

Murtagh, D., Frisk, U., Merino, F., Ridal, M., Jonsson, A., Stegman, J., Witt, G., Eriksson, P., Jimenez, C., Mégie, G., de la Noë, J., Ricaud, P., Baron, P., Pardo, J., Hauchcorne, A., Llewellyn, E., Degenstein, D., Gattinger, R., Lloyd, N., Evans, W., McDade, I., Haley, C., Sioris, C., von Savigny, C., Solheim, B., McConnell, J., Strong, K., Richardson, E., Leppelmeier, G., Kyrola, E., Auvinen, H., and Oikarinen, L.: An overview of the Odin atmospheric mission, Can. J. Phys., 80, 309–319, https://doi.org/10.1139/P01-157, 2002.

Ochiai, S., Baron, P., Nishibori, T., Irimajiri, Y., Uzawa, Y., Manabe, T., Maezawa, H., Mizuno, A., Nagahama, T., Sagawa, H., Suzuki, M., and Shiotani, M.: SMILES-2 Mission for Temperature, Wind, and Composition in the Whole Atmosphere, SOLA, 13A, 13–18, https://doi.org/10.2151/sola.13A-003, 2017.

Perrin, A., Puzzarini. C., Colmont, J.-M., Verdes, C., Wlodarczak, G., Cazzoli, G., Buehler, S., Flaud, J.-M., and Demaison, J.: Molecular Line Parameters for the "MASTER" (Millimeter Wave Acquisitions for Stratosphere/Troposphere Exchange Research) Database, J. Atmos. Chem, 51, 161-205, https://doi.org/10.1007/s10874-005-7185-9, 2005.

Pickett, H. M., Poynter, R. L., Cohen, E. A., Delitsky, M. L., Pearson, J. C., and Muller, H. S. P.: Submillimeter, millimeter, and microwave spectral line catalog, J. Quant. Spectrosc. Ra., 60, 883–890, https://doi.org/10.1016/S0022-4073(98)00091-0, 1998.

https://doi.org/10.5194/amt-2019-212
Preprint. Discussion started: 12 July 2019

Pumphrey, H. C., Santee, M. L., Livesey, N. J., Schwartz, M. J., and Read, W. G.: Microwave Limb Sounder observations of biomass-burning products from the Australian bush fires of February 2009, Atmos. Chem. Phys., 11, 6285-6296, https://doi.org/10.5194/acp-11-6285-2011, 2011.

Pumphrey, H. C., Read, W. G., Livesey, N. J., and Yang, K.: Observations of volcanic SO_2 from MLS on Aura, Atmos. Meas. Tech., 8, 195-209, https://doi.org/10.5194/amt-8-195-2015, 2015.

Rodgers, C. D.: Inverse Methods for Atmospheric Sounding: Theory and Practice, World Scientific, Singapore, 2000.

Rothman, L. S., Gordon, I. E., Babikov, Y., Barbe, A., ChrisBenner, D., Bernath, P. F., Birk, M., Bizzocchi, L., Boudon,V., Brown, L. R., Campargue, A., Chance, K., Cohen, E. A., Coudert, L. H., Devi, V. M., Drouin, B. J., Fayt, A., Flaud,J.-M., Gamache, R. R., Harrison, J. J., Hartmann, J. -M., Hill, C., Hodges, J. T., Jacquemart, D., Jolly, A., Lamouroux, J., Le Roy, R. J., Li, G., Long, D. A., Lyulin, O. M., Mackie, C. J., Massie, S. T., Mikhailenko, S., Müller, H. S. P., Nau-menko, O. V., Nikitin, A. V., Orphal, J., Perevalov, V., Per-rin, A., Polovtseva, E. R., Richard, C., Smith, M. A. H., Starikova, E., Sung, K., Tashkun, S., Tennyson, J., Toon, G. C., Tyuterev, V. G., and Wagner, G.: The HITRAN2012 molecular spectroscopic database, J. Quant. Spectrosc. Ra., 130, 4–50, https://doi.org/10.1016/j.jqsrt.2013.07.002, 2013.

Santee, M. L., Lambert, A., Read, W. G., Livesey, N. J., Manney, G. L., Cofield, R. E., Cuddy, D. T., Daffer, W. H., Drouin, B. J., Froidevaux, L., Fuller, R. A., Jarnot, R. F., Knosp, B. W., Perun, V. S., Snyder, W. V., Stek, P. C., Thurstans, R. P., Wagner, P. A., Waters, J. W., Connor, B., Urban, J., Murtagh, D., Ricaud, P., Barrett, B., Kleinböhl, A., Kuttippurath, J., Küllmann, H., von Hobe, M., Toon, G. C., and Stachnik, R. A.: Validation of the Aura Microwave Limb Sounder ClO measurements, J. Geophys. Res.-Atmos., 113, D15S22, https://doi.org/10.1029/2007JD008762, 2008.

Sato, T. O., Sagawa, H., Kreyling, D., Manabe, T., Ochiai, S., Kikuchi, K., Baron, P., Mendrok, J., Urban, J., Murtagh, D., Yasui, M., and Kasai, Y.: Strato-mesospheric ClO observations by SMILES: error analysis and diurnal variation, Atmos. Meas. Tech., 5, 2809-2825, https://doi.org/10.5194/amt-5-2809-2012, 2012.

Suzuki, M., Manago, N., Ozeki, H., Ochiai, S., and Baron, P.: Sensitivity study of smiles-2 for chemical species, in: Sensors, Systems, and Next-Generation Satellites XIX, Toulouse, France, 16 October 2015, 15, 2015.

Swadley, S. D., Poe, G. A., Bell, W., Hong, Y., Kunkee, D. B., McDermid, I. S., and Leblanc, T.: Analysis and Characterization of the SSMIS Upper Atmosphere Sounding Channel Measurements, IEEE T. Geosci. Remote, 46, 962–983, https://doi.org/10.1109/TGRS.2008.916980, 2008.

Takahashi, C., Ochiai, S., and Suzuki, M.: Operational retrieval algorithms for JEM/SMILES level 2 data processing system, J. Quant. Spectrosc. Ra., 111, 160–173, https://doi.org/10.1016/j.jqsrt.2009.06.005, 2010.

Takahashi, C., Suzuki, M., Mitsuda, C., Ochiai, S., Manago, N., Hayashi, H., Iwata, Y., Imai, K., Sano, T., Takayanagi, M., and Shiotani, M.: Capability for ozone high-precision retrieval on JEM/SMILES observation, Adv. Space Res., 48, 1076–1085, https://doi.org/10.1016/j.asr.2011.04.038, 2011.

Urban, J.: Optimal sub-millimeter bands for passive limb observations of stratospheric HBr, BrO, HOCl, and HO_2 from space, J. Quant. Spectrosc. Ra., 76, 145–178, https://doi.org/10.1016/s0022-4073(02)00051-1, 2003.

https://doi.org/10.5194/amt-2019-212
Preprint. Discussion started: 12 July 2019

Urban, J., Baron, P., Lautié, N., Schneider, N., Dassas, K., Ricaud, P., and De La Noë, J.: Moliere (v5): a versatile forward- and inversion model for the millimeter and sub-millimeter wavelength range, J. Quant. Spectrosc. Ra., 83, 529–554, https://doi.org/10.1016/S0022-4073(03)00104-3, 2004.

Urban, J., Lautié, N., Le Flochmoën, E., Jiménez, C., Eriksson, P., de La Noë, J., Dupuy, E., Ekström, M., El Amraoui, L., Frisk, U., Murtagh, D., Olberg, M., and Ricaud, P.: Odin/SMR limb observations of stratospheric trace gases: Level 2 processing of ClO, N_2O, HNO_3, and O_3, J. Geophys. Res.-Atmos., 110, D14307, https://doi.org/10.1029/2004JD005741, 2005.

Waters, J. W., Froidevaux, L., Read, W. G., Manney, G. L., Elson, L. S., Flower, D. A., Jarnot, R. F., and Harwood, R. S.: Stratospheric ClO and ozone from the Microwave Limb Sounder on the Upper Atmosphere Research Satellite, Nature, 362, 597–602, https://doi.org/10.1038/362597a0, 1993.

Waters, J.W., Froidevaux, L., Jarnot, R.F., Read, W.G., Pickett, H.M., Harwood, R.S., Cofield, R.E., Filipiak, M. J., Flower, D. A., Livesey, N. J., Manney, G. L., Pumphrey, H. C., Santee, M. L., Siegel, P. H., and Wu, D. L.: An Overview of the EOS MLS Experiment., Tech. Rep. JPL D-15745 / CL# 04-2323, Jet Propulsion Laboratory, California Institute of Technology, Pasadena, California, 91109-8099, available at: https://mls.jpl.nasa.gov/data/eos_overview_atbd.pdf (last access: 26 March 2019), Version 2.0, 2004.

Waters, J. W., Froidevaux, L., Harwood, R. S., Jarnot, R. F., Pickett, H. M., Read, W. G., Siegel, P. H., Cofield, R. E., Filipiak, M. J., Flower, D. A., Holden, J. R., Lau, G. K., Livesey, N. J., Manney, G. L., Pumphrey, H. C., Santee, M. L., Wu, D. L., Cuddy, D. T., Lay, R. R., Loo, M. S., Perun, V. S., Schwartz, M. J., Stek, P. C., Thurstans, R. P., Boyles, M. A., Chandra, K. M., Chavez, M. C., Chen, G.-S., Chudasama, B. V., Dodge, R., Fuller, R. A., Girard, M. A., Jiang, J. H., Jiang, Y., Knosp, B. W., LaBelle, R. C., Lam, J. C., Lee, K. A., Miller, D., Oswald, J. E., Patel, N. C., Pukala, D. M., Quintero, O., Scaff, D. M., Snyder, W. V., Tope, M. C., Wagner, P. A., and Walch, M. J.: The Earth Observing System Microwave Limb Sounder (EOS MLS) on the Aura Satellite, IEEE T. Geosci. Remote, 44, 1075–1092, https://doi.org/10.1109/TGRS.2006.873771, 2006.

Wu, D. L., Schwartz, M. J., Waters, J. W., Limpasuvan, V., Wu, Q., and Killeen, T. L.: Mesospheric doppler wind measurements from Aura Microwave Limb Sounder (MLS), Adv. Space Res., 42, 1246–1252, https://doi.org/10.1016/j.asr.2007.06.014, 2008.

Wu, D. L., Yee, J.-H., Schlecht, E., Mehdi, I., Siles, J., and Drouin, B. J.: THz limb sounder (TLS) for lower thermospheric wind, oxygen density, and temperature, J. Geophys. Res.-Space, 121, 7301–7315, https://doi.org/10.1002/2015JA022314, 2016.